A Mechanism for Regulation of Branched F-actin Networks by Dynamin2

Olga L. Askinazi
St. Petersburg, Russia

B.S., St. Petersburg State University, 2009
M.S., St. Petersburg State University, 2011

A Dissertation presented to the Graduate Faculty
of the University of Virginia in Candidacy for the Degree of
Doctor of Philosophy

Department of Biology

University of Virginia
May, 2018

_____

_____

_____

_____

_____

Abstract

Actin filaments assemble into networks with distinct architectures to support different actin-dependent processes. Despite their different organizations, filament networks are interdependent and often transition from one type to another in response to shifts in the balance of competing regulatory activities. Although we know a lot about actin and its assembly into different structures, we still do not understand what drives the assembly of specific network architectures in different parts of the cell and why and how assembled networks transition from one type of architecture to another.

The overarching goal of my research is to answer the question: How do complex actin filament networks form and exist in the cell? In Chapter 1 of this dissertation, I will discuss what we know about actin networks, regulation of their assembly and stability and how studying the role of a novel actin regulator, the large GTPase dynamin2 dynamin2 (dyn2) in actin regulation can help us answer essential questions about how dynamic actin filament (F-actin) networks form and provide cellular function.

In Chapter 2, I will present my experimental research on the mechanism by which dyn2 specifies the architecture of branched F-actin networks. Previous data suggested that dyn2 regulates branched actin filament networks within lamellipodia of migrating U2-OS cells to organize assembly of contractile actomyosin bundles at the lamella. Other data demonstrated that dyn2, in complex with cortactin, bundles actin filaments *in vitro*. Based on these findings, I hypothesized that dyn2 and cortactin specify the architecture of transient bundled structures in lamellipodia to assemble actomyosin bundles at the lamella. Using biochemical and microscopic assays with reconstituted F-actin networks

in vitro, I determined that dyn2, in complex with cortactin, bundles branched F-actin networks. Through the inhibition of F-actin nucleation, dyn2 promotes the formation of unbranched filaments that are subsequently bundled by a dyn2-cortactin complex. Dyn2/cortactin bundles selectively bind α-actinin, and GTP hydrolysis influences α-actinin binding to bundles. Together, these data provide a novel role for dyn2 and cortactin in promoting maturation of branched Arp2/3 complex-dependent networks into networks of filament bundles.

In Chapter 3, I propose a mechanism by which dyn2 regulates actin networks in lamellipodia to organize actomyosin assembly at the lamella and discuss future directions of this research. I speculate that transient dyn2/cortactin-dependent bundles in lamellipodia may co-assemble with myosin II filaments to promote the formation of actomyosin bundles at the lamella. The mechanism by which dyn2 bundles F-actin networks can be used in other cellular processes and structures where both Arp2/3 complex and dyn2 localize, such as endocytosis, exocytosis, phagocytosis, actin comets, filopodia, invadopodia, and cell-cell contacts.

Table of Contents

Acknowledgements and dedication

First, would like to thank my mentor, Dr. Dorothy Schafer who provided me with scientific guidance, advice, and support over the years. I also would like to thank the members of my thesis committee: Dr. Keith Kozminski, Dr. Bettina Winckler, Dr. Doug DeSimone, Dr. George Bloom, and Dr. Karsten Siller for helpful advice and interest in my project.

Thanks to all the former and current members of the Schafer and Kozminski labs, especially Dr. Manisha Menon who helped me a lot when I joined the lab. Thanks to many friends in St. Petersburg and Charlottesville who supported me all these years.

Finally, I'd like to dedicate this dissertation to my family who always believed in me more than I believed in myself: my parents and grandparents, my husband Matt and my daughter Hannah. Thank you and "spasibo" for your love and support.

List of abbreviations

ADF	Actin dissociating factor
Arp2/3	Actin-related protein 2/3
Dia2	Diaphanous-related formin 2
Dyn2	Dynamin2
Ena/VASP	Enabled/Vasodilator-stimulated phosphoprotein
F-actin	Filamentous actin
G-actin	Globular actin
GTPγS	Guanosine 5'-O-[gamma-thio]triphosphate
GMPPCP	Guanosine-5'-[(β,γ)-methyleno]triphosphate sodium salt
GMPPNP	5'-Guanylyl imidodiphosphate
NPF	Nucleation promoting factor
OCP	Osteoclast cell precursor
PH	Pleckstrin homology
PRD	Proline-rich domain
SH$_3$	Src homology three
EM	Electron microscopy
TIRF	Total internal reflection fluorescence
VCA	Verprolin, cofilin, acidic
WAVE	WASp family verprolin-homologous protein
WASp	Wiskott–Aldrich syndrome protein

Chapter 1. Introduction.

Dynamin2 as a regulator of F-actin networks

Cellular F-actin networks and their assembly.

Animal cells constantly change their shape in response to environmental cues. Dynamic shape changes are often and largely supported by assembly and disassembly of F-actin networks. Actin, a 42 kDa globular protein, assembles into filaments that, in turn, comprise networks of different types in different regions of a cell: sheet-like meshworks of crosslinked and branched networks in lamellipodia, tightly crosslinked filaments oriented in parallel within filopodia, and contractile actomyosin bundles that constitute transverse arcs and ventral stress fibers **(Fig. 1)**. The assembly of a specific actin network architecture is triggered by shifts in the balance of competing regulatory proteins. Assembled networks are interconnected and often transition from one type of organization to another. While actin and the dynamics of its turnover have been extensively studied, we still do not understand how actin filament networks assemble and exist in a changing cellular environment. In Chapter 1, I will describe different types of cellular actin networks, introduce dyn2 as an emerging regulator of branched F-actin networks, and present a rationale for my research.
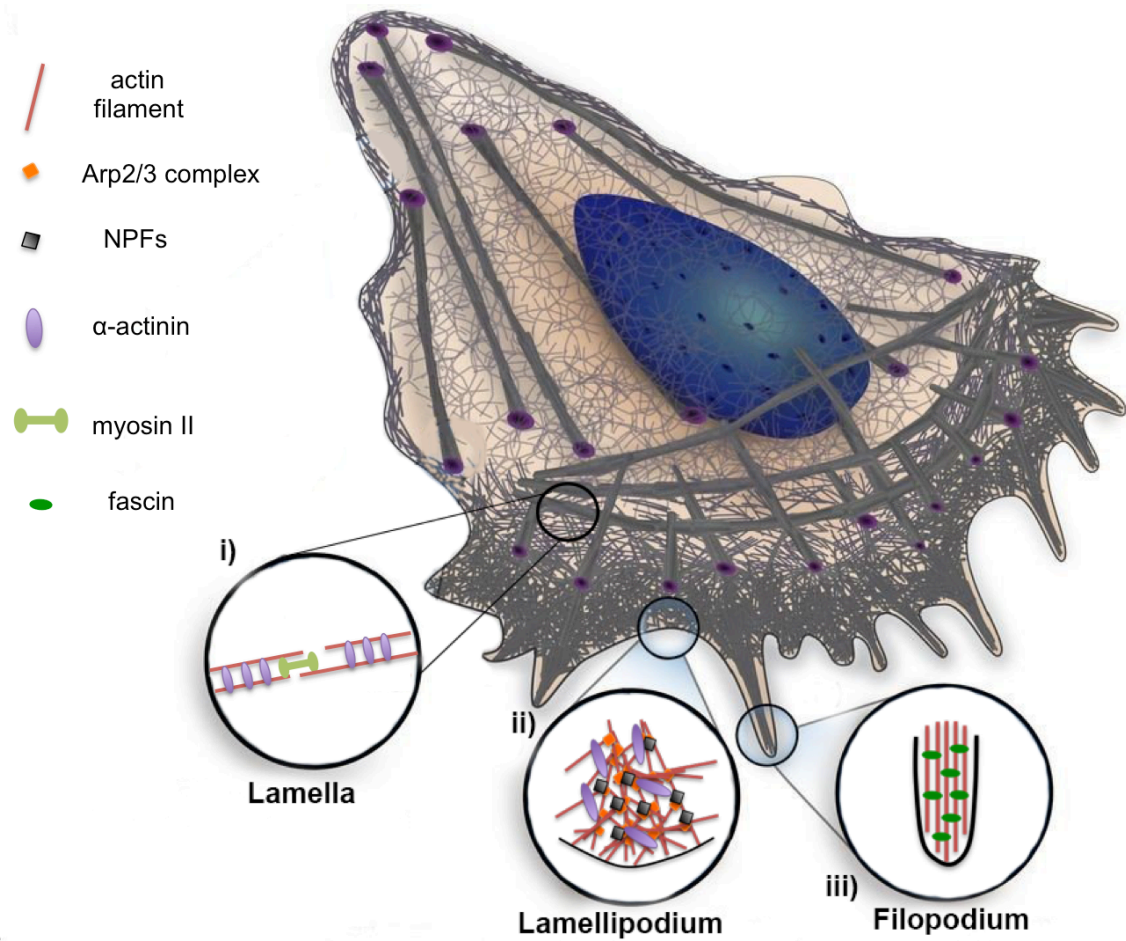
Figure 1. Actin architecture in a moving cell (modified from Blanchoin et al., 2014). The leading edge of the cell is in the bottom right. Actin structures in main figure are shown in gray (red in insets), focal adhesions are purple, and nucleus is blue.

i)   Antiparallel actomyosin bundles in transverse arcs of the lamella

ii) Branched Arp2/3 complex-dependent F-actin networks in lamellipodia (for clarity, Ena/VASP, capping protein, ADF/cofilin, and formin are not shown)

iii) Tightly crosslinked parallel filament bundles in filopodia

One of the most extensively studied actin networks in the cell is the branched network of lamellipodia, a quasi-two-dimensional network of dendritic F-actin beneath the membrane of the leading edge **(Fig. 1, ii).** The major nucleation factor involved in lamellipodia network assembly is Actin-related protein (Arp) 2/3 complex, which nucleates branched actin filament networks (Mullins et al., 1997). Arp2/3 complex is activated through interaction with its nucleation promoting factors (NPFs), among which are proteins of the Wiskott–Aldrich syndrome protein (WASp) family and cortactin (Campellone and Welch, 2010). Other major components of lamellipodial networks include crosslinkers, such as α-actinin; nucleators of non-branched actin filaments, called formins; the Enabled (Ena)/vasodilator-stimulated phosphoprotein (VASP) proteins, responsible for filament elongation; capping proteins; and proteins belonging to the family of actin disassembly factors (ADF)/cofilin (Ridley, 2011). All these proteins act in concert to promote actin assembly at the front edge of lamellipodia to drive forward membrane protrusion and recycle actin filaments.

Filopodia are long, thin cytoplasmic projections that extend beyond lamellipodia and serve as "antennae" to probe the environment during cell migration **(Fig. 1, iii)** (Mattila and Lappalainen, 2008). Filopodia contain tightly packed parallel bundles of actin filaments that are usually stabilized by a crosslinking protein, fascin. One model for filopodia assembly, called "convergent elongation," suggests that filopodia emerge from lamellipodial networks by gradual association of a subset of branched actin filaments decorated with Ena/VASP proteins (Svitkina et al., 2003). Association with Ena/VASP proteins protects the elongating barbed ends of actin filaments from capping and permits rapid polymerization, with subsequent bundling of elongated filaments by fascin. An alternate model for filopodia

formation involves the Diaphanous-related formin, Dia2 (Pellegrin and Mellor, 2005). In this model, filopodia arise as a result of *de novo* filament nucleation by Dia2, which *in vitro* performs all activities needed for filopodia formation: it nucleates linear actin filaments, accelerates actin polymerization, slows filament depolymerization, protects barbed ends from capping proteins, and bundles F-actin (Gupton and Gertler, 2007). It is unclear, however, whether this mechanism occurs *in vivo*.

Contractile actomyosin fibers constitute transverse arcs within the lamella **(Fig. 1, i)**, a region of the cell situated behind lamellipodia, and ventral stress fibers which run parallel to the direction of movement, linking focal adhesion sites. Both structures are responsible for coupling cellular actomyosin forces with the substrate to promote cell migration. Despite their unbranched structure, assembly of transverse arcs is partially dependent on Arp2/3 complex activity, and they assemble from branched networks at the lamellipodia-lamella interface (Burnette et al., 2011; Hotulainen and Lappalainen, 2006). Despite extensive research dedicated to the investigation of actomyosin assembly at the lamella, we still do not understand how actin filaments transition between lamellipodia and lamella, networks with such different architectures. My experimental research presented in Chapter 2 offers new insights that address this question.

Regulation of F-actin network assembly.

A developing view in the field of actin cytoskeleton is that multiple actin regulators compete for a finite pool of monomeric actin (G-actin) (Burke et al., 2014; Lomakin et al., 2015; Rotty et al., 2015; Suarez and Kovar, 2016). In the cell, the pool of G-actin is maintained at a constant level (Leavitt et al., 1987), which implies that the F-actin:G-

actin ratio is tightly regulated. Consequently, actin assembly is also homeostatic, and disruption of regulatory activities shifts the balance among F-actin networks of distinct morphologies competing for the same pool of G-actin. Specifically, depleting Arp2/3 complex dramatically increases the levels of formin-mediated F-actin cables in lamellipodia (Burke et al., 2014). In another study, genetic ablation of Arp2/3 complex in mammalian cells induced the formation of filopodia-like cables of parallel actin structures in lamellipodia, while the total level of F-actin remained unchanged (Rotty et al., 2015). Moreover, increasing the levels of profilin-1, a regulatory protein that binds actin monomers, disrupted lamellipodia and generated stress fiber-like structures, a phenotype consistent with the inhibition of the Arp2/3 complex activity and activation of formins. These studies suggest that different regulatory activities compete for a pool of actin monomers to create actin networks of distinct morphologies that under normal conditions are well balanced.

An additional layer of complexity is introduced when actin filaments assemble into networks. The three-dimensional organization of interconnected actin filaments imposes physical constraints that affect the assembly of higher-order F-actin structures. For example, in reconstituted actin networks formed *in vitro*, the F-actin crosslinker, α-actinin, only effectively bundled short, highly mobile actin filaments that were sufficiently diluted to avoid entanglement (Falzone et al., 2012). As actin polymerization proceeded, the rate of bundle formation slowed and eventually stopped, and networks became arrested as isotopic meshworks (mechanically resistive networks of interconnected filaments), suggesting that actin polymerization and bundling activities compete with each other.

Other data showed that inherent properties of actin crosslinkers (such as the distance between F-actin binding sites of the crosslinker and spacing between the crosslinker molecules on actin filaments) define the filament spacing in a bundle (Winkelman et al., 2016). This, in turn, enables the sorting of crosslinker molecules to specific filament structures; actin network bundled by α-actinin, for example, will favor binding of more α-actinin, but not fascin.

Together, these studies emphasize that kinetics of nucleation and filament assembly can determine which type of network will form. Consequently, the regulatory activities that manipulate the dynamics of actin nucleation or polymerization may promote the formation of a specific type of F-actin network. The search for factors that mediate the assembly of actin into different types of filament networks is ongoing. My experimental data presented in Chapter 2 suggest that dyn2 orchestrates the assembly of networks of filament bundles in the context of branched nucleation by Arp2/3 complex

Dyn2 and its role in regulating the assembly of F-actin networks.

Dynamin is a large 96 kDa GTPase **(Fig. 2)** that mediates membrane-remodeling processes. The "textbook" view is often focused on its action during scission of endocytic vesicles (Antonny et al., 2016; Ferguson and De Camilli, 2012). Dyn2 oligomers assemble around the necks of clathrin-coated pits that, following GTP hydrolysis, induce conformational changes that constrict the neck and trigger vesicle release from the membrane. In a cell-free system, dynamin and GTP are sufficient to constrict the necks of lipid tubules (Sweitzer and Hinshaw, 1998), making this GTPase unique in its ability to act as a mechanochemical enzyme. Cellular data, however, indicate that vesicle fission is

dependent on several other proteins (Antonny et al., 2016), and the exact mechanism

of fission remains to be investigated.
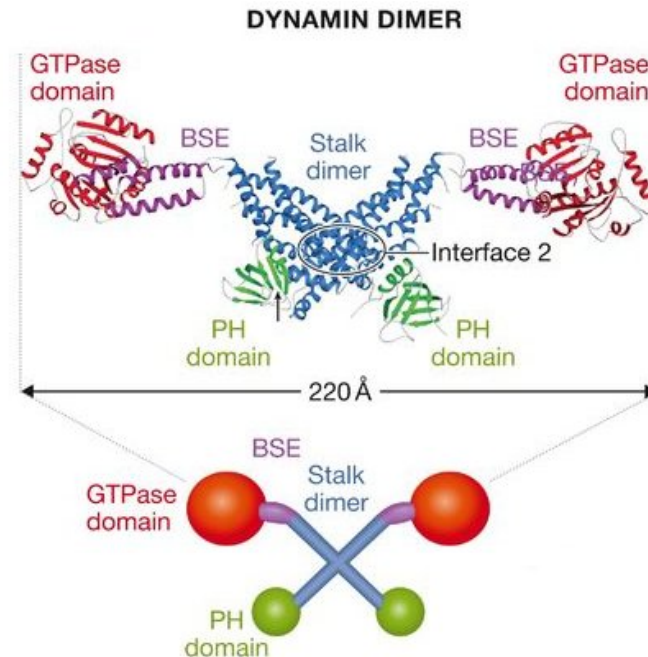
Figure 2. Domain structure of the crystalized dynamin dimer (from Antonny et al., 2016; Ford et al., 2011). Proline-rich domain (PRD) is not shown because it has not been crystallized.

There are three mammalian isoforms of dynamin: dynamin1, enriched in neuronal tissues

where it is involved in presynaptic vesicle endocytosis, the ubiquitous isoform dynamin2

(dyn2), and brain-localized dynamin3, which is responsible for synaptic vesicle recycling

(Cook et al., 1996; Sontag et al., 1994; Tanifuji et al., 2013). Additionally, each dynamin

isoform has at least four splice variants (Cao et al., 1998). The focus of this dissertation is

on the dyn2 due to its ubiquitous nature.

Substantial evidence suggests that endocytic fission depends on actin (Boulant et al., 2011; Lamaze et al., 1997; Yarar et al., 2004). Dyn2 colocalizes spatially and temporally with the endocytic actin machinery, including Arp2/3 complex, N-WASp, and cortactin (Merrifield et al., 2002, 2004, 2005). Dynamin1 was shown to control actin dynamics at sites of endocytosis in NIH-3T3 cells (Taylor et al., 2012). Interaction of actin and yeast dynamin homolog, Vps1, is required for vesicle scission because mutations in Vps1 that affected F-actin binding also disrupt endocytosis (Palmer et al., 2015). Vps1 also formed ring-like oligomeric structures that bundled F-actin *in vitro*, and mutations in the actin-binding repeats in the Vps1 stalk domain inhibited bundle formation, but not ring assembly. These data suggest that Vps1 oligomers promote the formation of F-actin bundles at the neck of the clathrin-coated pits, and filament bundles may transduce the force of actin polymerization to the membrane to drive successful scission.

Beyond endocytosis, dyn2 is implicated in regulating the assembly of several actin structures and actin-driven processes across the cell such as actin comets, membrane ruffles, filopodia, phagocytic cups, podosomes, invadopodia, actomyosin rings in epithelial cells, exocytosis, cell-cell fusion, and lamellipodia **(Table 1)** (Anantharam et al., 2011; Chua et al., 2009; Destaing et al., 2013; Gold et al., 1999; Lee and De Camilli, 2002; McNiven et al., 2000, 2004; Menon et al., 2014; Shin et al., 2014; Yamada et al., 2013). *In vitro*, dyn2 directly binds actin filaments (Gu et al., 2010) and, together with cortactin, bundles them (Mooren et al., 2009). Interestingly, a common feature of all known F-actin structures and processes where dyn2 is enriched is the presence of Arp2/3 complex-dependent branched F-actin networks **(Table 1).** Therefore, studying how dyn2

regulates the actin cytoskeleton is necessary to understand the principles of assembly and reorganization of complex F-actin networks. In the following section, I will summarize proposed molecular mechanisms of dyn2 action on actin filaments.

Actin structure/ process	Dependence on Arp2/3 complex?	Enrichment in cortactin?	Dyn2-cortactin interaction required for dyn2 function?	Dyn2 function depends on GTPase activity?	References
Endocytosis	Yes	Yes	Yes	Yes	Palmer et al., 2015; Taylor et al., 2012
Actin comets	Yes	Yes	Possible*	Yes	Lee and De Camilli, 2002; Orth et al., 2002
Filopodia	Yes	Yes	Yes	Yes	Yamada et al., 2013, 2016a
Phagocytic cups	Yes	Yes	Not shown	Yes	Gold et al., 1999; Otsuka et al., 2009
Membrane ruffles	Yes	Yes	Yes	Not shown	Krueger et al., 2003
Podosomes and invadopodia	Yes	Yes	Not shown	Yes	Destaing et al., 2013; Ochoa et al., 2000; Zhang et al., 2016
Actomyosin networks	Yes	Yes	Yes	Yes	Chua et al., 2009; Mooren et al., 2009
Exocytosis	Yes	Yes	Not shown	Yes	Anantharam et al., 2011; Jaiswal et al., 2009; Lasič et al., 2017
Cell-cell fusion	Yes	Yes	Not shown	Yes	Leikina et al., 2013; Shin et al., 2014
Lamellipodia	Yes	Yes	Possible*	Yes	Menon et al., 2014; Yamada et al., 2009, 2016b

Table 1. Types of actin structures or processes that depend on dyn2 and their common features. *The PRD of dyn2 was shown to be indispensable for the dyn2 function

Dyn2 and actin biochemistry

Despite the advantages of studies conducted *in vivo*, it is often challenging to separate dyn2 function in the scission of endocytic vesicles from its effects on actin regulation. As an alternative, experiments performed with purified proteins *in vitro* provide insights into the molecular mechanisms by which dyn2 regulates actin dynamics and network organization.

Studies from our lab first implicated dyn2 in regulating F-actin *in vitro* based on observations that dyn2 influenced F-actin nucleation by Arp2/3 complex and cortactin, as observed by bulk F-actin assembly using pyrenyl-actin (Schafer et al., 2002). Regulation of branched network assembly by dyn2 was dependent on the interaction between dyn2 and cortactin because replacing wild type cortactin for cortactin-W525K, a mutant form that has a decreased affinity to dyn2, did not alter actin assembly.

Later studies showed that dyn2 in complex with cortactin bundles actin filaments, as observed by negative stain transmission electron microscopy (EM) experiments and total internal reflection fluorescence (TIRF) microscopy **(Fig. 3)** (Mooren et al., 2009). The extent of filament bundling was dependent on dyn2 GTPase activity because replacing GTP with a non-hydrolyzable GTP analog, GTPγS, changed the organization of the bundles, making them more tightly packed. Additionally, cortactin, but not cortactin-W525K, enhanced the intrinsic GTPase activity of unassembled dyn2 and stabilized the association of dyn2 with actin filaments, as shown by low-speed centrifugation assays. These data support the idea that the dyn2-cortactin interaction and dyn2 GTPase activity are involved in dyn2-dependent effects on actin filaments.
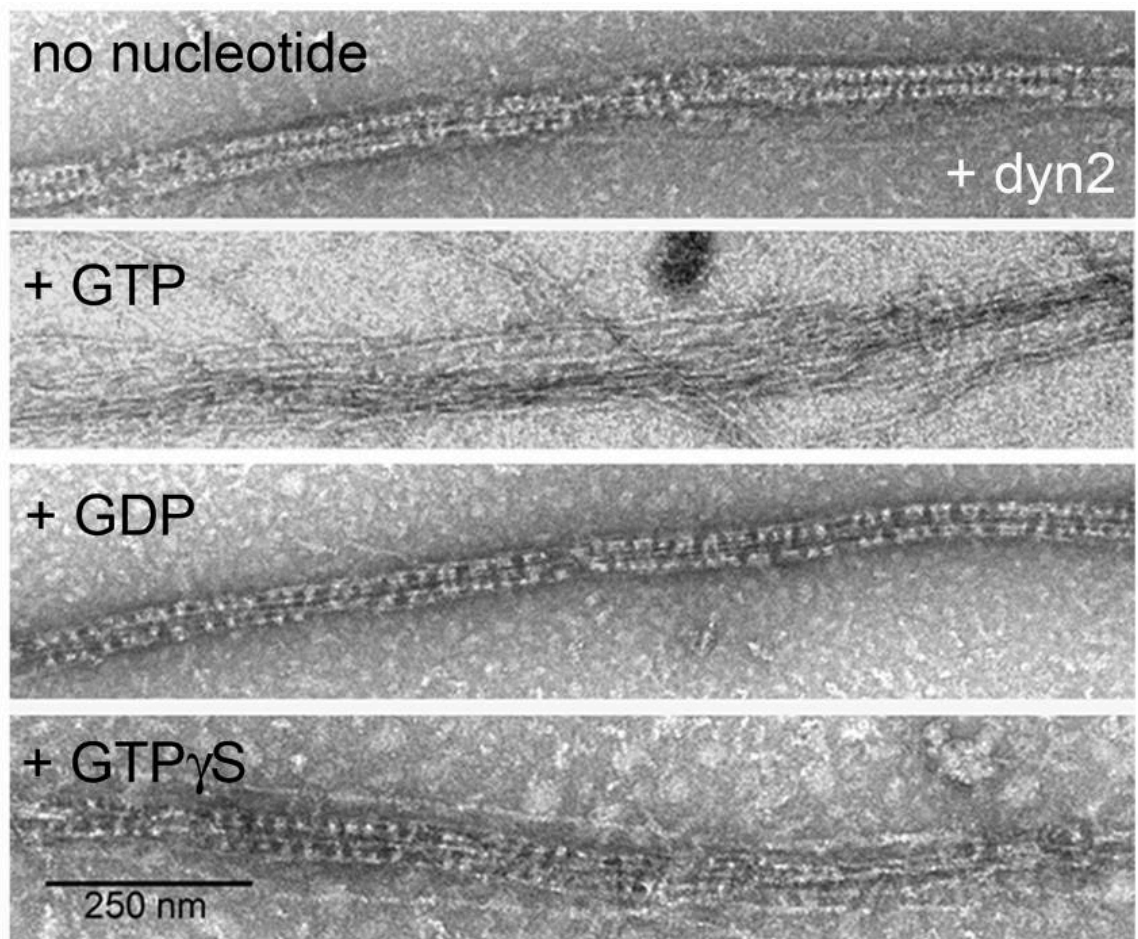
Figure 3. Dyn2 and cortactin bundle actin filaments. Transmission electron micrograph of F-actin bundles assembled by dyn2 and cortactin, with addition of different guanine nucleotides, as indicated (from Mooren et al., 2009)

Gu et al. (2010) also showed that dynamin1 directly bundles actin filaments *in vitro*; however, in their system, dynamin1 acted independently of cortactin. F-actin-binding site was mapped to a region between amino acids 399 and 444 of the stalk domain of dynamin1; this region contains several positively-charged amino acids that are conserved from yeast to mammals. Dynamin oligomerization regulated bundling because addition of GTPγS, which induces dynamin oligomerization, changed the structure of bundles, making them more regular. *In vivo*, dynamin oligomers induced by dynamin activator, Ryngo, were detected on the cell membrane and at sites of transition between cortical actin networks and stress fibers, suggesting a role for dynamin oligomerization in membrane and actin-driven processes across the cell (Gu et al., 2014).

Taken together, these data suggest that dyn2 GTPase, potentially with cortactin, bundle actin filaments *in vitro*. Although we do not know the exact function of dyn2 in actin processes and structures in the cell, *in vitro* findings provide potential mechanisms on how dyn2 regulates cellular F-actin networks. In the following sections of the introduction I will discuss cellular structures and processes that require dyn2, focusing on what is known about the role of dyn2 in regulating actin network dynamics, and present a rationale for my research.

Dyn2 in actin comet networks

Actin comets are actin structures formed by some species of intracellular pathogenic bacteria or viruses. Actin comets power bacteria movement within the cytoplasm of infected host cells or from one host cell to the next. Dyn2 is associated with actin tails of *Listeria monocytogenes* where it regulates actin assembly (Lee and De Camilli, 2002). Actin comets

also can be induced by expressing type I phosphatidylinositol 4-phosphate 5-kinase; in

induced comet tails, the mutant form dyn2-K44A, which is defective in GTP binding and

hydrolysis, reduced the number of comet-forming vesicles and largely decreased comet

length and velocity of movement, indicating that dyn2 GTPase regulates actin assembly in

tails (Orth et al., 2002). The proline-rich domain (PRD) of dyn2 targeted it to the comet tail

and regulated actin dynamics in the tails. The PRD links dyn2 to other proteins such as

cortactin to which it binds through a Src homology three (SH_3) domain (McNiven et al.,

2000). Interestingly, cortactin is also a component of actin tails (Orth et al., 2002).

Therefore, it is possible that dyn2 regulates actin assembly in comet tails together with

cortactin. F-actin in tails is nucleated by Arp2/3 complex but, unexpectedly, cryo-electron

micrographs of *Listeria* tails formed *in vivo* reveal tightly-packed bundles (Jasnin et al.,

2013). Because dyn2 and cortactin bundle actin filaments *in vitro* (Mooren et al., 2009), it is

possible that dyn2 and cortactin in actin tails assemble Arp2/3 complex-dependent networks

into bundled structures.

Dyn2 in filopodial bundles

Formation of filopodia also depends on dynamin and cortactin (Yamada et al., 2013,

2016a). Neurons extend filopodial protrusions from growth cones. A "ring" complex of

dynamin1 and cortactin mechanically stabilized F-actin bundles in growth cones via a GTP-

dependent mechanism (Yamada et al., 2013). Specifically, ring-like structures of dynamin1

and cortactin, observed by negative stain EM, appeared "open" or "closed" depending on

the presence of hydrolyzable guanine nucleotide. Yamada et al. (2013) proposed a model, in

which GTP hydrolysis by dynamin1 closes dynamin1-cortactin rings, acting like a "cinch"

that brings actin filaments together to create filament bundles. Similar dyn2-cortactin complexes stabilized filpopodia in human non-small carcinoma cells facilitating cell migration and metastatic growth (Yamada et al., 2016a). Knockdown of dyn2 or cortactin resulted in a loss of actin bundles and inhibited filopodia formation. As discussed earlier, filopodia are thought to initiate from branched Arp2/3 complex-dependent actin networks in lamellipodia (Svitkina et al., 2003). Therefore, it is possible that dyn2-cortactin complex reorganizes Arp2/3 complex-dependent branched filaments into bundled structures that elongate to form lamellipodia.

Dyn2 in podosomes and invadopodia

Podosomes and invadopodia are actin-rich membrane protrusions that attach and degrade extracellular matrix to facilitate cell motility and invasion (Gimona et al., 2008). By convention, the term *podosomes* refers to the structures in normal cells, while usually longer *invadopodia* are found in cancer cells. Actin filaments in these structures are arranged into bundles oriented perpendicularly to the substrate and surrounded by a "cloud" of branched Arp2/3 complex-dependent F-actin parallel to the substrate (Luxenburg et al., 2007).

Dyn2 is essential for podosomes/invadopodia assembly, stability, and migration/invasion (Destaing et al., 2013; Ochoa et al., 2000; Zhang et al., 2016). Dyn2 is proposed to regulate actin turnover via a GTPase-dependent mechanism: dominant-negative dyn2 K44A mutant that is defective in GTP binding and hydrolysis displayed a decreased rate of F-actin turnover (Ochoa et al., 2000). Interestingly, dyn2 function in podosomes requires a full-length protein, suggesting that it is dependent on coordinated activity of its membrane-binding pleckstrin homology (PH), PRD, and GTPase domains **(Fig. 2)**

(Baldassarre et al., 2003; Destaing et al., 2013). In invadopodia, PRD and GTPase domains were essential for the function of dyn2 (Zhang et al., 2016).

Cortactin also regulates the assembly and maturation of invadopodia (Oser et al., 2009). Specifically, Förster resonance energy transfer experiments showed that phosphorylated cortactin binds the actin-binding protein cofilin and promotes cofilin's severing activity. Severing of actin filaments increases the number of barbed ends to promote actin assembly and formation of invadopodia. Dephosphorylation releases cortactin from cofilin and inhibits severing, which stabilizes the assembled structure. Therefore, dyn2 and cortactin may play a role in assembling bundled structures that constitute the core of podosomes and invadopodia from a branched F-actin "cloud."

Dyn2 in phagocytic cups and membrane ruffles

Dyn2 is implicated in the formation of membrane structures such as protrusions extended during phagocytosis by macrophages and Sertoli cells (Gold et al., 1999; Otsuka et al., 2009) and cortical ruffles, large circular structures on the dorsal surface of cells, formed in response to growth factor stimulation (Krueger et al., 2003). Similar to other dyn2-dependent processes, both structures rely on Arp2/3 complex-dependent branched F-actin networks. Recruitment of dyn2 to actin networks in ruffles depended on interactions with cortactin through the PRD of dyn2. Inhibition of dyn2 and/or cortactin arrested formation of these protrusive structures, suggesting that a dyn2-cortactin complex may be involved in establishing and maintaining the actin networks underlying protrusions.

Dyn2 in actomyosin networks

Dyn2 is implicated in regulating actomyosin networks found in the lamellae of migrating cells and in contracting actin belts in epithelial cells during morphogenesis (Chua et al., 2009; Menon et al., 2014). Depletion of dyn2 caused epithelial cells to lose polarity and tight junctions (Chua et al., 2009). Additionally, expression of the GTP binding mutant, dyn2-K44A, resulted in apical constriction, a phenotype dependent on myosin II activity. These data indicate that GTP hydrolysis by dyn2 modulates actomyosin contractility in the apical region of epithelial cells. Interestingly, a cortactin mutant defective in dyn2 binding when co-expressed with dyn2-K44A prevented apical constriction, suggesting that dyn2-K44A modulates the actomyosin contractile machinery to trigger apical constriction through interactions with cortactin.

At the lamella, dyn2 depletion in U2-OS cells disrupted formation of nascent actomyosin structures. Dyn2 loss increased retrograde flow of myosin II puncta that assembled together to generate contractile actomyosin bundles (Menon et al., 2014). Interestingly, dyn2 is not localized at the lamella; rather, it is situated at the protruding edge of lamellipodia. Therefore, dyn2 is proposed to regulate actomyosin assembly indirectly through its effects on lamelipodial F-actin networks. This finding highlights the interdependence of different F-actin networks in the cell.

Dyn2 and exocytosis

Dynamin is implicated in membrane remodeling during exocytosis (Anantharam et al., 2011; Jaiswal et al., 2009; Lasič et al., 2017). Specifically, dynamin1 GTPase activity was shown to control expansion of the fusion pore (a structure that connects two membrane

compartments during their fusion) (Anantharam et al., 2011). A mutant dynamin1 with increased rate of GTP hydrolysis triggered rapid fusion pore expansion after exocytosis. Conversely, a dynamin1 mutant with decreased GTPase rate slowed fusion pore expansion. More recently, it was shown that dynamin oligomerization also modulates fusion pore kinetics (Lasič et al., 2017). Specifically, pharmacological inhibitors Dyngo and Dynole, which affect GTP binding, caused fusion pore to lapse into a non-functional "flickering" state (repetitive opening and closing). The actin cytoskeleton that underlies the process of exocytosis and fusion pore expansion is dependent on Arp2/3 complex and cortactin (González-Jamett et al., 2017; Porat-Shliom et al., 2013). Whether the complex of dyn2 and cortactin and its interaction with actin filaments are involved in controlling the fusion pore dynamics during exocytosis remains to be investigated.

Dyn2 in cell-cell fusion

Recently, dyn2 has been implicated in fusion of myoblasts into multinucleated myotubes during muscle development and regeneration (Leikina et al., 2013) and fusion of osteoclast precursors (OCPs) into multinucleated osteoclast cells for bone resorption (Shin et al., 2014). The earlier stages of cell fusion involve hemifusion, or merging of outer membrane leaflets, and the later stages involve merging of inner leaflets of the membranes to form and expand the fusion pore. The dyn2 inhibitor, Dynasore, that locks dyn2 in a GTP-bound state, and dyn2 depletion altered later stages of myoblast fusion (Leikina et al., 2013). Dyn2 activity and phosphatidylinositol 4,5-bisphosphate, an activator of dyn2 GTPase (Lin et al., 1997), were required for syncytium formation, the last step of cell fusion. Although the mechanism by which dyn2 functions during myoblast fusion is not known, it may be

similar to its function during exocytosis where dyn2 is also implicated in regulating fusion pore dynamics.

In another study, inducible knockouts of dynamin1 and dyn2 disrupted fusion of OCPs and myoblasts and prevented formation of multinucleated osteoclasts and myotubes, respectively (Shin et al., 2014). Depletion of both dynamin isoforms inhibited the formation of long podosome-like actin-rich protrusions normally observed between fusing cells. Dynamin activity required the presence of the PRD, PH, and GTPase domains **(Fig. 2)**, suggesting that their interplay in creating a functional dynamin oligomer is crucial for fusion events. Interestingly, clathrin-mediated endocytosis was also required for cell-cell fusion. Therefore, it is possible that the role of dynamin in the fusion process involves both the formation of actin-rich structures at sites of cell-cell fusion, ensuring close contact between the membranes of fusing cells (Sens et al., 2010), and the process of endocytosis.

Like other processes involving dyn2, cell-cell fusion is powered by branched Arp2/3-complex dependent networks (Berger et al., 2008; Chen et al., 2007). In *Drosophila*, Arp2/3 complex in fusion sites is activated by WAVE (WASp family verprolin-homologous protein) and WASp. Arp2/3 complex and cortactin have both been colocalized with the actin-rich zipper-like structures that "seal" neighboring cells during osteoclast fusion (Takito et al., 2012). It is of interest to test whether dyn2 and cortactin reorganize actin filaments during cell-cell fusion.

Dyn2 in lamellipodia

Actin filaments of lamellipodia power advancement of the leading edge by applying pushing forces of polymerizing actin on the plasma membrane **(Fig. 1)**. Several research groups have implicated dyn2 in regulating the branched Arp2/3 complex-dependent networks in lamellipodia (McNiven et al., 2000; Menon et al., 2014; Mooren et al., 2009; Yamada et al., 2009, 2016b).

Dyn2 was implicated in regulating lamellipodial actin networks based on the fact that pharmacological inhibition of dyn2 with Dynasore suppressed serum-induced lamellipodia extension in U2-OS cells (Yamada et al., 2009). In this system, dyn2 colocalized with both actin and cortactin, and Dynasore partially disrupted those associations. However, Dynasore and other dynamin inhibitors have off-target effects in direct inhibition of some actin processes (Park et al., 2013). An alternative to using Dynasore is dyn2 depletion through knockdown or inducible knockout.

Studies from our lab showed that dyn2 is localized at the edge of advancing lamellipodial protrusions, possibly through its interaction with cortactin or other proteins and direct binding to actin filaments (Menon et al., 2014). Depletion of dyn2 in U2-OS cells increased the width of lamellipodia and altered the spatio-temporal distribution of the F-actin crosslinker, α-actinin, and its engagement with maturing focal adhesions. Dyn2 depletion also affected assembly of contractile actomyosin arcs at the lamella in the GTPase-dependent manner, as described earlier.

Recent data have highlighted the role of specific sites in *DNM2* (gene that encodes dyn2) in the process of lamellipodia formation (Yamada et al., 2016b). Specifically, the mutants that affect the Pleckstrin homology (PH) domain of dyn2 and are associated with

Charcot-Marie-Tooth disease (inherited peripheral neuropathy), dyn2-555Δ3 and dyn2-K562E, caused 50% decrease in serum-dependent lamellipodia formation in U2-OS and HeLa cells. Interestingly, expression of dyn2-K562E caused loss of transverse F-actin bundles and formation of actin clusters, which correlated with aberrant F-actin dynamics observed by live-cell imaging.

Together, data presented in this section highlight a role for dyn2 and cortactin in assembling several F-actin-dependent structures and processes. Data from *in vitro* experiments presented earlier offer potential mechanisms for how dyn2 acts in cellular processes. Because all known processes where dyn2 and cortactin are enriched are dependent on Arp2/3 complex and dyn2 and cortactin bundle actin filaments *in vitro*, I hypothesize that dyn2 in complex with cortactin potentiate the formation of bundled F-actin structures in the context of branched Arp2/3 complex-dependent networks.


Rationale for the study

Studying how different types of actin architecture transition from one to another is important for our understanding of how the actin cytoskeleton functions as a whole. In this dissertation, I dissect the mechanism by which dyn2 bundles actin filaments within the branched Arp2/3 complex-dependent F-actin networks **(Fig. 4)**. Previous data from our lab showed that (1) dyn2, together with cortactin and in a GTPase-dependent manner, bundles actin filaments *in vitro* (Mooren et al., 2009) and (2) dyn2 depletion alters the spatio-temporal distribution of actin crosslinker, α-actinin, in lamellipodia and perturbs assembly of actomyosin bundles in the lamella of U2-OS cells (Menon et al., 2014). Together, these data lead to a hypothesis that lamellipodial dyn2 and cortactin locally

specify the architecture of bundled F-actin structures that give rise to nascent actomyosin bundles of the lamella. Specifically, dyn2 and cortactin may generate a collection of short bundled actin filaments (a "template") in lamellipodia that may be ideally suited for crosslinking by α-actinin and/or myosin II. It was previously proposed that α-actinin and myosin II associate with actin filaments in lamellipodia to generate actomyosin bundles at the lamella (Burnette et al., 2011; Hotulainen and Lappalainen, 2006). By generating "bundle templates" within branched F-actin networks of lamellipodia, dyn2 and cortactin can indirectly regulate the assembly of transverse F-actin arcs at the lamella.

To dissect the mechanism by which dyn2 and cortactin bundle F-actin, I use biochemical and microscopic approaches to visualize reconstituted branched F-actin networks formed with or without dyn2 and cortactin. I determine the minimum components that promote F-actin bundling, determine factors that enhance or inhibit bundle assembly, and propose a mechanism by which dyn2 creates a bundle template. Finally, using fluorescently labeled proteins, I determine whether dyn2-dependent bundles bind the filament crosslinker, α-actinin.
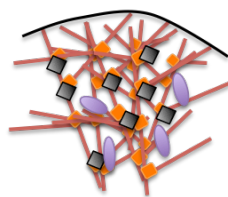
Figure 4. Model of relationship between lamellipodial F-actin networks and lamellar actomyosin at inception of this study.

References

Anantharam, A., Bittner, M. A., Aikman, R.L., Stuenkel, E.L., Schmid, S.L., Axelrod, D., and Holz, R.W. (2011). A new role for the dynamin GTPase in the regulation of fusion pore expansion. Mol. Biol. Cell *22*, 1907–1918.

Antonny, B., Burd, C., De Camilli, P., Chen, E., Daumke, O., Faelber, K., Ford, M., Frolov, V.A., Frost, A., Hinshaw, J.E., et al. (2016). Membrane fission by dynamin: what we know and what we need to know. EMBO J. *35*, 2270–2284.

Baldassarre, M., Pompeo, A., Beznoussenko, G., Castaldi, C., Cortellino, S., McNiven, M.A., Luini, A., and Buccione, R. (2003). Dynamin Participates in Focal Extracellular Matrix Degradation by Invasive Cells. Mol. Biol. Cell *14*, 1074–1084.

Barroso, C., Rodenbusch, S.E., Welch, M.D., and Drubin, D.G. (2006). A role for cortactin in *Listeria monocytogenes* invasion of NIH 3T3 cells, but not in its intracellular motility. Cell Motil. Cytoskeleton *63*, 231–243.

Berger, S., Schafer, G., Kesper, D.A., Holz, A., Eriksson, T., Palmer, R.H., Beck, L., Klambt, C., Renkawitz-Pohl, R., and Onel, S.-F. (2008). WASP and SCAR have distinct roles in activating the Arp2/3 complex during myoblast fusion. J. Cell Sci. *121*, 1303–1313.

Blanchoin, L., Boujemaa-Paterski, R., Sykes, C., and Plastino, J. (2014). Actin dynamics, architecture, and mechanics in cell motility. Physiol. Rev. *94*, 235–263.

Boulant, S., Kural, C., Zeeh, J.C., Ubelmann, F., and Kirchhausen, T. (2011). Actin dynamics counteract membrane tension during clathrin-mediated endocytosis. Nat. Cell Biol. *13*, 1124–1132.

Burke, T. A., Christensen, J. R., Barone, E., Suarez, C., Sirotkin, V., and Kovar, D. R. (2014). Homeostatic actin cytoskeleton networks are regulated by assembly factor competition for monomers. Curr. Biol. *24*, 579–585.

Burnette, D.T., Manley, S., Sengupta, P., Sougrat, R., Davidson, M.W., Kachar, B., and Lippincott-Schwartz, J. (2011). A role for actin arcs in the leading-edge advance of migrating cells. Nat. Cell Biol. *13*, 371–381.

Campellone, K.G., and Welch, M.D. (2010). A nucleator arms race: Cellular control of actin assembly. Nat. Rev. Mol. Cell Biol. *11*, 237–251.

Cao, H., Garcia, F., and Mcniven, M. A. (1998). Differential distribution of dynamin isoforms in mammalian cells. Mol. Biol. Cell *9*, 2595–2609.

Chen, E.H., Grote, E., Mohler, W., and Vignery, A. (2007). Cell-cell fusion. FEBS Lett. *581*, 2181–2193.

Chua, J., Rikhy, R., and Lippincott-Schwartz, J. (2009). Dynamin 2 orchestrates the global actomyosin cytoskeleton for epithelial maintenance and apical constriction. Proc. Natl. Acad. Sci. *106*, 20770–20775.

Cook, T., Mesa, K., and Urrutia, R. (1996). Three dynamin-encoding genes are differentially expressed in developing rat brain. J. Neurochem. *67*, 927–931.

Destaing, O., Ferguson, S.M., Grichine, A., Oddou, C., De Camilli, P., Albiges-Rizo, C., and Baron, R. (2013). Essential Function of Dynamin in the Invasive Properties and Actin Architecture of v-Src Induced Podosomes/Invadosomes. PLoS One *8*, e77956.

Falzone, T.T., Lenz, M., Kovar, D.R., and Gardel, M.L. (2012). Assembly kinetics determine the architecture of α -actinin crosslinked F-actin networks. Nat. Commun. *3*, 861–869.

Ferguson, S.M., and De Camilli, P. (2012). Dynamin, a membrane-remodelling GTPase. Nat. Rev. Mol. Cell Biol. *13*, 75–88.

Ford, M.G.J., Jenni, S., and Nunnari, J. (2011). The crystal structure of dynamin. Nature *477*, 561–566.

Gimona, M., Buccione, R., Courtneidge, S.A., and Linder, S. (2008). Assembly and biological role of podosomes and invadopodia. Curr. Opin. Cell Biol. *20*, 235–241.

Gold, E.S., Underhill, D.M., Morrissette, N.S., Guo, J., McNiven, M. a, and Aderem, a (1999). Dynamin 2 is required for phagocytosis in macrophages. J. Exp. Med. *190*, 1849–1856.

González-Jamett, A.M., Guerra, M.J., Olivares, M.J., Haro-Acuña, V., Baéz-Matus, X., Vásquez-Navarrete, J., Momboisse, F., Martinez-Quiles, N., and Cárdenas, A.M. (2017). The F-Actin Binding Protein Cortactin Regulates the Dynamics of the Exocytotic Fusion Pore through its SH3 Domain. Front. Cell. Neurosci. *11*, 130.

Goode, B.L., Rodal, A.A., Barnes, G., and Drubin, D.G. (2001). Activation of the Arp2/3 complex by the actin filament binding protein Abp1p. J. Cell Biol. *152*, 627–634.

Grassart, A., Cheng, A.T., Hong, S.H., Zhang, F., Zenzer, N., Feng, Y., Briner, D.M., Davis, G.D., Malkov, D., and Drubin, D.G. (2014). Actin and dynamin2 dynamics and interplay during clathrin-mediated endocytosis. J. Cell Biol. *205*, 721–735.

Gu, C., Yaddanapudi, S., Weins, A., Osborn, T., Reiser, J., Pollak, M., Hartwig, J., and Sever, S. (2010). Direct dynamin-actin interactions regulate the actin cytoskeleton.

EMBO J. *29*, 3593–3606.

Gu, C., Chang, J., Shchedrina, V.A., Pham, V.A., Hartwig, J.H., Suphamungmee, W., Lehman, W., Hyman, B.T., Bacskai, B.J., and Sever, S. (2014). Regulation of dynamin oligomerization in cells: The role of dynamin-actin interactions and its GTPase activity. Traffic *15*, 819–838.

Gupton, S.L., and Gertler, F.B. (2007). Filopodia: the fingers that do the walking. Sci. STKE *2007*, re5.

Hotulainen, P., and Lappalainen, P. (2006). Stress fibers are generated by two distinct actin assembly mechanisms in motile cells. J. Cell Biol. *173*, 383–394.

Jaiswal, J.K., Rivera, V.M., and Simon, S.M. (2009). Exocytosis of post-Golgi vesicles is regulated by components of the endocytic machinery. Cell *137*, 1308–1319.

Jasnin, M., Asano, S., Gouin, E., Hegerl, R., Plitzko, J.M., Villa, E., Cossart, P., and Baumeister, W. (2013). Three-dimensional architecture of actin filaments in Listeria monocytogenes comet tails. Proc. Natl. Acad. Sci. *110*, 20521–20526.

Krueger, E.W., Orth, J.D., Cao, H., and McNiven, M.A. (2003). A dynamin-cortactin-Arp2/3 complex mediates actin reorganization in growth factor-stimulated cells. Mol. Biol. Cell *14*, 1085–1096.

Lamaze, C., Fujimoto, L.M., Yin, H.L., and Schmid, S.L. (1997). The actin cytoskeleton is required for receptor-mediated endocytosis in mammalian cells. J. Biol. Chem. *272*, 20332–20335.

Lasič, E., Stenovec, M., Kreft, M., Robinson, P.J., and Zorec, R. (2017). Dynamin regulates the fusion pore of endo- and exocytotic vesicles as revealed by membrane capacitance measurements. Biochim. Biophys. Acta - Gen. Subj. *1861*, 2293–2303.

Leavitt, J., Ng, S.Y., Aebi, U., Varma, M., Latter, G., Burbeck, S., Kedes, L., and Gunning, P. (1987). Expression of transfected mutant beta-actin genes: alterations of cell morphology and evidence for autoregulation in actin pools. Mol. Cell. Biol. *7*, 2457–2466.

Lee, E., and De Camilli, P. (2002). Dynamin at actin tails. Proc. Natl. Acad. Sci. *99*, 161–166.

Leikina, E., Melikov, K., Sanyal, S., Verma, S.K., Eun, B., Gebert, C., Pfeifer, K., Lizunov, V.A., Kozlov, M.M., and Chernomordik, L. V. (2013). Extracellular annexins and dynamin are important for sequential steps in myoblast fusion. J. Cell Biol. *200*, 109–123.

Lin, H.C., Barylko, B., Achiriloaie, M., and Albanesi, J.P. (1997). Phosphatidylinositol (4,5)-bisphosphate-dependent activation of dynamins I and II lacking the proline/arginine-rich domains. J. Biol. Chem. *272*, 25999–26004.

Lomakin, A.J., Lee, K.-C.C., Han, S.J., Bui, D.A., Davidson, M., Mogilner, A., and Danuser, G. (2015). Competition for actin between two distinct F-actin networks defines a bistable switch for cell polarization. Nat. Cell Biol. *17*, 1435-1445.

Luxenburg, C., Geblinger, D., Klein, E., Anderson, K., Hanein, D., Geiger, B., and Addadi, L. (2007). The architecture of the adhesive apparatus of cultured osteoclasts: From podosome formation to sealing zone assembly. PLoS One *2*, e179.

Mattila, P.K., and Lappalainen, P. (2008). Filopodia: Molecular architecture and cellular functions. Nat. Rev. Mol. Cell Biol. *9*, 446–454.

McNiven, M.A., Kim, L., Krueger, E.W., Orth, J.D., Cao, H., and Wong, T.W. (2000). Regulated interactions between dynamin and the actin-binding protein cortactin modulate cell shape. J. Cell Biol. *151*, 187–198.

McNiven, M.A., Baldassarre, M., and Buccione, R. (2004). The role of dynamin in the assembly and function of podosomes and invadopodia. Front Biosci *9*, 1944–1953.

Menon, M., Askinazi, O.L., and Schafer, D.A. (2014). Dynamin2 organizes lamellipodial actin networks to orchestrate lamellar actomyosin. PLoS One *9*, e94330.

Merrifield, C.J., Feldman, M.E., Wan, L., and Almers, W. (2002). Imaging actin and dynamin recruitment during invagination of single clathrin-coated pits. Nat. Cell Biol. *4*, 691–698.

Merrifield, C.J., Qualmann, B., Kessels, M.M., and Almers, W. (2004). Neural Wiskott Aldrich Syndrome Protein (N-WASP) and the Arp 2/3 complex are recruited to sites of clathrin-mediated endocytosis in cultured fibroblasts. Eur. J. Cell Biol. *83*, 13–18.

Merrifield, C.J., Perrais, D., and Zenisek, D. (2005). Coupling between clathrin-coated-pit invagination, cortactin recruitment, and membrane scission observed in live cells. Cell *121*, 593–606.

Mooren, O., Kotova, T., Moore, A., and Schafer, D. (2009). Dynamin2 GTPase and cortactin remodel actin filaments. J. Biol. Chem. *284*, 23995–24005.

Mullins, R.D., Stafford, W.F., and Pollard, T.D. (1997). Structure, subunit topology, and actin-binding activity of the Arp2/3 complex from Acanthamoeba. J. Cell Biol. *136*, 331–343.

Ochoa, G., Slepnev, V.I., Neff, L., Ringstad, N., Takei, K., Daniell, L., Kim, W., Cao, H.,

McNiven, M., Baron, R., et al. (2000). A Functional Link between Dynamin and the Actin Cytoskeleton at Podosomes. *150*, 377–389.

Orth, J.D., Krueger, E.W., Cao, H., and McNiven, M. a (2002). The large GTPase dynamin regulates actin comet formation and movement in living cells. Proc. Natl. Acad. Sci. *99*, 167–172.

Oser, M., Yamaguchi, H., Mader, C.C., Bravo-Cordero, J.J., Arias, M., Chen, X., DesMarais, V., Van Rheenen, J., Koleske, A.J., and Condeelis, J. (2009). Cortactin regulates cofilin and N-WASp activities to control the stages of invadopodium assembly and maturation. J. Cell Biol. *186*, 571–587.

Otsuka, A., Abe, T., Watanabe, M., Yagisawa, H., Takei, K., and Yamada, H. (2009). Dynamin 2 is required for actin assembly in phagocytosis in Sertoli cells. Biochem. Biophys. Res. Commun. *378*, 478–482.

Palmer, S.E., Smaczynska-de Rooij, I.I., Marklew, C.J., Allwood, E.G., Mishra, R., Johnson, S., Goldberg, M.W., and Ayscough, K.R. (2015). A Dynamin-Actin Interaction Is Required for Vesicle Scission during Endocytosis in Yeast. Curr. Biol. *25*, 868–878.

Park, R.J., Shen, H., Liu, L., Liu, X., Ferguson, S.M., and De Camilli, P. (2013). Dynamin triple knockout cells reveal off target effects of commonly used dynamin inhibitors. J. Cell Sci. *126*, 5305–5312.

Pellegrin, S., and Mellor, H. (2005). The Rho family GTPase Rif induces filopodia through mDia2. Curr. Biol. *15*, 129–133.

Porat-Shliom, N., Milberg, O., Masedunskas, A., and Weigert, R. (2013). Multiple roles for the actin cytoskeleton during regulated exocytosis. Cell. Mol. Life Sci. *70*, 2099–2121.

Ridley, A.J. (2011). Life at the leading edge. Cell *145*, 1012–1022.

Rotty, J.D., Wu, C., Haynes, E.M., Suarez, C., Winkelman, J.D., Johnson, H.E., Haugh, J.M., Kovar, D.R., and Bear, J.E. (2015). Profilin-1 Serves as a gatekeeper for actin assembly by Arp2/3-Dependent and - Independent pathways. Dev. Cell *32*, 54–67.

Schafer, D.A., Weed, S.A., Binns, D., Karginov, A. V., Parsons, J.T., and Cooper, J.A. (2002). Dynamin2 and cortactin regulate actin assembly and filament organization. Curr. Biol. *12*, 1852–1857.

Sens, K.L., Zhang, S., Jin, P., Duan, R., Zhang, G., Luo, F., Parachini, L., and Chen, E.H. (2010). An invasive podosome-like structure promotes fusion pore formation during myoblast fusion. J. Cell Biol. *191*, 1013–1027.

Shin, N.-Y., Choi, H., Neff, L., Wu, Y., Saito, H., Ferguson, S.M., De Camilli, P., and Baron, R. (2014). Dynamin and endocytosis are required for the fusion of osteoclasts and myoblasts. J. Cell Biol. *207*, 73–89.

Sontag, J.M., Fykse, E.M., Ushkaryov, Y., Liu, J.P., Robinson, P.J., and Südhof, T.C. (1994). Differential expression and regulation of multiple dynamins. J. Biol. Chem. *269*, 4547–4554.

Suarez, C., and Kovar, D.R. (2016). Internetwork competition for monomers governs actin cytoskeleton organization. Nat. Rev. Mol. Cell Biol. *17*, 799–810.

Svitkina, T.M., Bulanova, E.A., Chaga, O.Y., Vignjevic, D.M., Kojima, S. ichiro, Vasiliev, J.M., and Borisy, G.G. (2003). Mechanism of filopodia initiation by reorganization of a dendritic network. J. Cell Biol. *160*, 409–421.

Sweitzer, S.M. and Hinshaw, J.E. (1998). Dynamin undergoes a GTP-dependent conformational change causing vesiculation. Cell *93*, 1021–1029.

Takito, J., Nakamura, M., Yoda, M., Tohmonda, T., Uchikawa, S., Horiuchi, K., Toyama, Y., and Chiba, K. (2012). The transient appearance of zipper-like actin superstructures during the fusion of osteoclasts. J. Cell Sci. *125*, 662–672.

Tanifuji, S., Funakoshi-Tago, M., Uedas, F., Kasaharas, T., and Mochida, S. (2013). Dynamin isoforms decode action potential firing for synaptic vesicle recycling. J. Biol. Chem. *288*, 19050–19059.

Taylor, M.J., Lampe, M., and Merrifield, C.J. (2012). A feedback loop between dynamin and actin recruitment during clathrin-mediated endocytosis. PLoS Biol. *10*, e1001302.

Winkelman, J.D., Suarez, C., Hocky, G.M., Harker, A.J., Morganthaler, A.N., Christensen, J.R., Voth, G.A., Bartles, J.R., and Kovar, D.R. (2016). Fascin- and α-Actinin-Bundled Networks Contain Intrinsic Structural Features that Drive Protein Sorting. Curr. Biol. *26*, 2697–2706.

Yamada, H., Abe, T., Li, S.-A.A., Masuoka, Y., Isoda, M., Watanabe, M., Nasu, Y., Kumon, H., Asai, A., and Takei, K. (2009). Dynasore, a dynamin inhibitor, suppresses lamellipodia formation and cancer cell invasion by destabilizing actin filaments. Biochem. Biophys. Res. Commun. *390*, 1142–1148.

Yamada, H., Abe, T., Satoh, A., Okazaki, N., Tago, S., Kobayashi, K., Yoshida, Y., Oda, Y., Watanabe, M., Tomizawa, K., et al. (2013). Stabilization of Actin Bundles by a Dynamin 1/Cortactin Ring Complex Is Necessary for Growth Cone Filopodia. J. Neurosci. *33*, 4514–4526.

Yamada, H., Takeda, T., Michiue, H., Abe, T., and Takei, K. (2016a). Actin bundling by

dynamin 2 and cortactin is implicated in cell migration by stabilizing filopodia in human non-small cell lung carcinoma cells. Int. J. Oncol. *49*, 877–886.

Yamada, H., Kobayashi, K., Zhang, Y., Takeda, T., and Takei, K. (2016b). Expression of a dynamin 2 mutant associated with Charcot-Marie-Tooth disease leads to aberrant actin dynamics and lamellipodia formation. Neurosci. Lett. *628*, 179–185.

Yarar, D., Waterman-Storer, C.M., and Schmid, S.L. (2004). A Dynamic Actin Cytoskeleton Functions at Multiple Stages of Clathrin-mediated Endocytosis. Mol. Biol. Cell *16*, 964–975.

Zhang, Y., Nolan, M., Yamada, H., Watanabe, M., Nasu, Y., Takei, K., and Takeda, T. (2016). Dynamin2 GTPase contributes to invadopodia formation in invasive bladder cancer cells. Biochem. Biophys. Res. Commun. *480*, 409–414.

Chapter 2.

Dynamin2 and cortactin specify the architecture of branched actin networks by tuning actin nucleation and crosslinking filaments

Askinazi OL, Schafer DA (2018). Dynamin2 and cortactin specify the architecture of branched actin networks by tuning actin nucleation and crosslinking filaments. *Mol Biol Cell* (submitted).

Abstract

Cellular F-actin networks assemble with diverse architectures and can change their structures as cells move, divide and transport intracellular cargoes. Many actin binding proteins direct assembly of actin filaments in distinct network morphologies, but mechanisms for spatial and temporal changes in actin filament organization required for cellular processes are poorly understood. Dynamin2 is enriched in branched actin networks, but its depletion from cells disrupted both branched networks of lamellipodia and bundled actomyosin networks of lamellae. To determine how dynamin2 acts on branched actin filaments we assembled branched networks *in vitro*. Dynamin2 promotes filament bundling within Arp2/3 complex-dependent networks via two mechanisms. First, dynamin2 interferes with actin nucleation, creating unbranched filaments. Second, dynamin2, in concert with cortactin, crosslink actin filaments in mixed-polarity bundles. We propose that a complex of dynamin2 and cortactin bind and align short, unbranched actin filaments, creating a "bundle template" that directs formation of bundled filaments. Interestingly, bundled filaments generated by dyn2 and cortactin selectively bind the actin filament crosslinker, α-actinin. These findings identify roles for dyn2 and cortactin in locally tuning the architecture of actin filaments, leading to structural polymorphisms that confer distinct mechanical properties and structures to cellular actin networks.

Introduction

Cellular actin networks are constructed in different architectures designed to support varied cellular processes: sheet-like meshworks of short, branched actin filaments exert protrusive forces on membranes; uniformly-oriented, aligned filaments tightly crosslinked as bundles within filopodia protrude and probe the environment; and arrays of loosely-packed, crosslinked actin filaments and motor proteins generate tensile forces to shape and move cells and govern cellular interactions within tissues. All these networks are spatially and temporally dynamic and interdependent. For example, filaments originating within branched actin networks are recruited to form axially-arrayed, bundled filaments of filopodia (Svitkina *et al.*, 2003). On the other hand, filaments arising from branched actin networks co-assemble with filaments of myosin II, generating contractile actomyosin networks of lamellae and at adherens junctions (Hotulainen and Lappalainen, 2006; Burnette *et al.*, 2011; Michael *et al.*, 2016). Investigating how different types of F-actin networks assemble and become integrated to form a coherent, global actin cytoskeleton is required to understand the physiological roles of actin.

In cells, actin network morphology is determined by the balance of actin nucleation activity, actin assembly kinetics, the type and concentrations of crosslinking proteins that stabilize networks and the presence of filament motor proteins. Ample evidence implicates the actions of key actin nucleating proteins, Arp2/3 complex and formins, among others, in specifying overall network architecture as primarily branched or bundled (reviewed in Chhabra and Higgs, 2007). An emerging view is that distinct actin network architectures arise from competition by nucleating proteins for a finite pool of

monomeric actin as modulated by the activity of profilin (Burke *et al.*, 2014; Lomakin *et al.*, 2015; Rotty *et al.*, 2015; Suarez and Kovar, 2016). Generating distinct network architectures also requires spatially orienting actin filaments with respect to one another and to other cellular structures within a crowded cytoplasm. Although actin nucleating factors can specify filament arrangements, physical constraints in dense networks can restrict assembly of higher-order F-actin structures. For example, in reconstituted actin networks formed *in vitro*, the filament crosslinker, α-actinin effectively crosslinks short, mobile actin filaments as bundles, but filament bundling by α-actinin is decreased in favor of crosslinking filaments as a meshwork when filaments are long, entangled and less mobile (Falzone *et al.*, 2012). Actin filament crosslinking proteins also possess intrinsic distances between their F-actin binding motifs that define the spacing of filaments within crosslinked structures. Hence, once bundling of aligned filaments is initiated by interactions with a specific crosslinker, filament spacing can be propagated as bundles expand via filament elongation and concomitant crosslinker binding (Winkelman *et al.*, 2016).

Cellular experiments have implicated the large GTPase dynamin2 (dyn2) in regulating filament dynamics and organization in several contexts, particularly within branched actin networks (Lee and De Camilli, 2002; Chua *et al.*, 2009; Ferguson *et al.*, 2009; Gu *et al.*, 2010; Anantharam *et al.*, 2011; Destaing *et al.*, 2013; Leikina *et al.*, 2013; Menon *et al.*, 2014; Palmer *et al.*, 2015). Dyn2 and its binding partner, cortactin, colocalize within many Arp2/3 complex-dependent branched actin networks formed *in vivo* (McNiven *et al.*, 2000; Lee and De Camilli, 2002; Orth *et al.*, 2002; Schafer *et al.*, 2002; Krueger *et al.*, 2003). In U2-OS cells, dyn2 is localized at the edge of protruding,

but not retracting, segments of the plasma membrane, where it influences lamellipod

width, the spatiotemporal organization of components of lamellipodial actin networks,

assembly of nascent actomyosin, and accumulation of α-actinin at maturing focal

adhesions (Menon *et al.*, 2014). Dynamin isoforms and cortactin each directly bind F-

actin (Wu and Parsons, 1993; Gu *et al.*, 2010) and regulate actin nucleation by Arp2/3

complex *in vitro* (Weaver *et al.*, 2001; Schafer *et al.*, 2002). Other work demonstrated

that dynamin isoforms also bundle actin filaments *in vitro*, although the conditions for

bundling varied (Mooren *et al.*, 2009; Gu *et al.*, 2010; Yamada *et al.*, 2013). Together,

these findings led us to hypothesize that dyn2 bundles a subset of actin filaments within

Arp2/3 complex-dependent branched actin networks to establish higher-order actin

networks such as actomyosin and filopodial bundles.

To test this hypothesis, we assembled branched actin networks *in vitro* from pure

components. We found that dyn2 antagonizes actin nucleation by Arp2/3 complex and,

with cortactin, generates bundled actin filaments within branched actin networks.

Because dyn2 influenced the spatiotemporal distribution of α-actinin within

lamellipodia and the assembly of nascent actomyosin, which is stabilized by α-actinin

(Mooren *et al.*, 2009; Menon *et al.*, 2014), we investigated a role for dyn2 in generating

a network of bundles suited for binding α-actinin. Unexpectedly, the association of α-

actinin with dyn2-dependent bundles was decreased compared to its association with α-

actinin-dependent bundles, suggesting that dyn2 and cortactin generate a bundled

filament architecture that limits binding of α-actinin. Our results contribute to

understanding how structural polymorphisms are introduced locally within actin

networks to give rise to the complex, interconnected and coherent actin cytoskeleton found in cells.

Results

<u>Dyn2 competes with branched actin nucleation to generate bundled F-actin</u>

To determine how dyn2 influences filament organization within branched actin networks, we assembled networks nucleated by Arp2/3 complex and nucleation promoting factors (NPFs) in the absence or presence of varying concentrations of dyn2. F-actin networks were observed using time-lapse confocal microscopy of Alexa647-phalloidin-labeled actin filaments (see Materials and Methods). F-actin formed in reactions containing Arp2/3 complex, GST-VCA (a GST fusion of the catalytic NPF domain of N-WASp) and cortactin were detected within 2-5 min as focal, diffuse structures **(Fig. 1A, upper panel, Video1).** Over time the focal F-actin assemblies increased in size and Alexa647-phalloidin intensity, but they remained diffuse with no apparent structure as expected for branched actin filaments in solution observed at the resolution achieved by confocal microscopy. Addition of 130 nM dyn2 to the network reactions resulted in appearance of brightly-stained elongate structures, presumably bundled actin filaments, within regions of diffuse F-actin **(Fig. 1A, Video1)**. Actin networks formed in reactions containing higher concentrations of dyn2 were predominately bundled. At concentrations of dyn2 >400 nM, the brightly-stained bundled actin structures appeared interconnected throughout the three-dimensional sample volume **(Fig. 1A, Video1).**

To assess filament bundling by dyn2 in these networks, we quantified the extent of filament bundling and the F-actin content of bundles over time **(Fig. 1B, C)**. F-actin bundles were identified as maxima of Alexa647-phalloidin fluorescence above a designated threshold along line scans obtained at each timepoint **(Fig. S1A, B)**; bundle density was defined as the number of peaks per μm along the lines. F-actin content of bundles was obtained from the maximum intensity of Alexa647-phalloidin fluorescence of each peak. Using these criteria, no bundled structures were detected in networks containing Arp2/3 complex and NPFs **(Fig. 1B)**. In networks containing dyn2, bundle density and average F-actin content in bundled structures increased over time and plateaued by ~15 min **(Fig. 1B,C)**. Bundle density and F-actin content in bundles depended on the concentration of dyn2 **(Fig. 1D)**. These data show that the presence of dyn2 in F-actin networks nucleated by Arp2/3 complex, GST-VCA, and cortactin changes network organization from predominately branched to predominantly bundled. Bundled F-actin structures were detected within minutes in reactions containing dyn2, before diffuse, branched F-actin was apparent **(Fig. S1C)**. Together, these data suggest that dyn2 competes with filament branching to promote formation of bundled actin filaments within reconstituted actin networks generated by Arp2/3 complex.

Filament bundling by dynamin2 requires cortactin

Cortactin is a NPF for Arp2/3 complex that binds both actin filaments and dyn2 (McNiven *et al.*, 2000; Weed *et al.*, 2000; Weaver *et al.*, 2001). Cortactin and dyn2 were previously shown to promote actin filament bundling *in vitro* (Mooren *et al.*, 2009) and cortactin was recently shown to enhance branched nucleation activity by

Arp2/3 complex in synergy with VCA-containing NPFs (Helgeson and Nolen, 2013).

We confirmed a requirement for cortactin for dyn2-dependent bundling in reconstituted actin networks using a mutant form of cortactin, cortactin-W525K, that does not bind the dyn2 proline-rich domain (PRD) (McNiven *et al.*, 2000; Schafer *et al.*, 2002). No bundled actin structures formed in networks containing dyn2 and cortactin-W525K; only diffuse, focal F-actin structures, characteristic of branched actin, were observed **(Fig. 2A, B; Video2)**. Interestingly, filament bundling by dyn2 and cortactin was also robust in the absence of branched nucleation activity **(Fig. 2C, D, Video3)**. Spontaneously nucleated actin filaments assembled as long, interconnected F-actin bundles in reactions containing dyn2 and wild type cortactin. In contrast, spontaneous actin assembly in reactions with dyn2 and cortactin-W525K, or lacking cortactin altogether, yielded uniformly-diffuse F-actin networks, unlike the focal, diffuse F-actin structures generated by Arp2/3 complex, GST-VCA and cortactin. Although the cortactin N-terminal F-actin repeats are reported to bundle actin filaments when branch density is low (Helgeson *et al.*, 2014), interactions of dyn2 and cortactin were required for filament bundling in our reconstituted networks. These data show that dyn2 and cortactin act together to promote filament bundling within branched and unbranched actin networks *in vitro*.

GTP hydrolysis by dyn2 influences the morphology of F-actin networks

GTP hydrolysis by dyn2 influences its conformation and oligomerization dynamics (Warnock *et al.*, 1996; Hinshaw, 2000; Marks *et al.*, 2001; Chappie *et al.*, 2011; Anand *et al.*, 2016), thus, our reconstituted networks generally contained 1.5 mM GTP. To

explore a role for GTP binding and hydrolysis by dyn2 in specifying actin network morphology, we either omitted GTP or used the non-hydrolyzable analog, GMPPCP. Actin filaments formed in reactions containing 1.5 mM GMPPCP were predominately bundled, but bundles were shorter and appeared less interconnected than those formed in the presence of GTP **(Fig. 3; Video4)**. Bundled structures also formed in the absence of guanine nucleotide but, unlike the interconnected network of bundles that formed in the presence of GTP, bundled structures were isolated, appeared disorganized and contained, on average, less F-actin **(Fig. 3B,C)**. These data show that GTP hydrolysis by dyn2 regulates the spatial organization of F-actin bundles formed within reconstituted actin networks nucleated by Arp2/3 complex.

Dyn2 slows the rate of actin nucleation *in vitro*

We sought to determine the mechanism by which dyn2 and cortactin promote filament bundling within branched actin networks. The earliest F-actin structures observed in reconstituted networks containing dyn2 appeared as small bundled structures (Fig. S1C); diffuse F-actin characteristic of branched filaments was not observed at early times. This observation suggests that dyn2 and cortactin interfere with actin nucleation by Arp2/3 complex and promote bundling of unbranched actin filaments. By antagonizing branched actin nucleation, dyn2 and cortactin could crosslink spontaneously nucleated actin filaments to form bundled structures. An alternate hypothesis is that dyn2 and cortactin bind to branched filament junctions and promote unbranching coincident with crosslinking the remodeled filaments as a bundle.

Previous biochemical studies indicated that dyn2 inhibited bulk actin assembly by Arp2/3 complex and cortactin (Schafer *et al.*, 2002). We confirmed that dyn2 also inhibits actin assembly by Arp2/3 complex, GST-VCA and cortactin using assays that monitored fluorescence of pyrenyl-actin; the time for half-maximal polymerization, relative to that in the absence of dyn2, increased in a manner that depended on the concentration of dyn2 **(Fig. 4A, B)**. In contrast with its requirement for filament bundling, inhibition of Arp2/3 complex-dependent actin nucleation by dyn2 did not require cortactin **(Fig S2A-C)**. Dyn2 also inhibited spontaneous actin assembly but did not alter the rate of actin polymerization initiated by spectrin-actin seeds (SAS) or the steady state critical concentration for actin assembly **(Fig. S2D-F)**. Together, these data show that dyn2 delays actin nucleation but does not cap filament barbed ends, sequester actin monomer, or alter the rate of filament elongation at barbed ends. We suggest that dyn2 inhibits Arp2/3 complex-dependent actin nucleation by decreasing formation of mother filaments and by direct effects on branched actin nucleation by Arp2/3 complex.

To determine if dyn2 and cortactin directly inhibit branched nucleation by Arp2/3 complex, we quantified Arp2/3 complex-dependent filament branching in the presence and absence of dyn2 using TIRF microscopy **(Fig. 4C-F, Fig. S3)**. Consistent with the results of bulk solution assays of actin assembly, dyn2, with or without cortactin, delayed the appearance of branched filaments and decreased the amount of F-actin formed at early times in these reactions **(Fig. 4C-F, Fig. S3)**. The presence of GTP or GMP-PNP slightly, but not significantly, decreased filament branching in reactions containing dyn2 compared to reactions with no added guanine nucleotide **(Fig. 4D, Fig. S3B)**. These data confirm that dyn2 decreases the rate of branched actin nucleation by

Arp2/3 complex *in vitro*. Decreased branched nucleation could promote filament bundling by creating linear actin filaments poised for crosslinking. Importantly, bundling of filaments at or near branched filament junctions was not observed in the TIRF movies, indicating that dyn2 and cortactin do not appear to actively remodel filaments at branched junctions to generate linear filaments that align and crosslink. Nonetheless, we cannot rule out that filament remodeling at branched junctions is constrained for filaments observed using TIRF microcopy due to their close proximity to the chamber surface.

Dyn2 and cortactin direct formation of parallel and anti-parallel filament bundles

To further examine the mechanisms for filament bundling and to determine the polarity of filaments within bundles formed by dyn2 and cortactin, we observed interactions of individual filaments using TIRF microscopy. Interestingly, although bundled structures sometimes fell from solution into the evanescent wave at later times in these reactions, most bundles observed using TIRF microscopy formed as a consequence of interactions of elongating filaments and coincident crosslinking; bundled F-actin structures were not commonly observed at early times, even when reactions were pre-incubated for 2-3 minutes before flowing into the sample chamber.

Filament bundling occurred as elongating filaments collided with other filaments and continued to elongate, tracking along the contacted filaments to create 2-(or more)-filament bundles (**Fig. 5A).** The fraction of bundles containing two or more filaments in reactions containing dyn2, cortactin and GTP increased over time **(Fig. 5C, Video5a)**. In contrast, although bundled filaments formed in reactions containing dyn2 and either

cortactin-W525K or wild type cortactin with GMPPNP, the fraction of bundled filaments remained constant over the duration of the timelapse movie **(Fig. 5C)**. The decreased extent of bundling in reactions containing cortactin-W525K or GMPPNP is supported by the shorter duration of individual filament tracking events compared to those in reactions containing wild type cortactin and GTP (see below; Fig. 5D). In control reactions lacking dyn2, individual filaments collided and interacted via their sides to form small regions of 2-filament bundles, but most filament interactions were transient and few stable bundled structures formed during the duration of the timelapse movie **(Fig. S4; Video5b)**.

To determine the relative orientations of interacting filaments and the duration of filament-on-filament tracking events, we analyzed how bundles formed via collisions and binding interactions **(Fig. 5B, D)**. Many filaments became bundled after collisions of their elongating barbed ends with the sides of other filaments; in this case, the colliding barbed end shifted direction to continue elongating along the filament with which it had interacted. Such end-to-side collisions created 2-filament bundles in which filaments were oriented either in parallel (cyan asterisks in Fig. 5B) or anti-parallel (yellow asterisks in Fig. 5B), depending on the relative orientations of the colliding filaments. In other cases, two elongating filaments encountered each other head-on via their growing barbed ends; each filament continued to elongate along the other, creating an anti-parallel, 2-filament bundle. Continued collisions and interactions of filaments over time led to formation of bundled structures with 3 or more filaments. The number of bundled structures with parallel or anti-parallel filament orientations was equal under all conditions **(Fig. 5D)**. The average duration of filament-on-filament tracking that

propagated bundles was nearly 2-fold longer for filaments in reactions containing dyn2, cortactin and GTP (151.44±5.99 s, n=124) compared to that in reactions containing either cortactin-W525K (84.2±3.5 s, n=82) or GMPPCP (77±3.49 s, n=76) **(Fig 5D)**. Occasionally, a new filament nucleated on an existing filament and continued to elongate along the filament without forming an apparent branched junction. This observation suggests that addition of new filaments to existing bundles can also occur via *de novo* nucleation within the bundle itself, as well as via interactions of elongating filaments with other filaments.

Dyn2 regulates recruitment of α-actinin to bundled F-actin

Cellular experiments implicated dyn2 in regulating the association of α-actinin with lamellipodial and lamellar actin networks and at focal adhesions in U2-OS cells (Mooren *et al.*, 2009; Menon *et al.*, 2014). Based on these findings, we hypothesized that, by specifying filament architecture, dyn2 and cortactin also specify interactions of bundled filaments and actin filament crosslinkers, such as α-actinin. To test this hypothesis, we quantified the association of Alexa555-α-actinin-4 (hereafter referred to as α-actinin) with bundled filaments formed in reconstituted actin networks. Other studies showed that high rates of branching nucleation inhibit filament bundling by actin crosslinkers, most likely due to the steric constraints of aligning branched filaments (Skau *et al.*, 2011; Helgeson *et al.*, 2014). Consistent with these findings, a threshold concentration of 200 nM α-actinin was required to detect any bundled filaments in reconstituted actin networks in the absence of dyn2 **(Fig. S5A, upper panels)**. Small bundled structures were embedded within diffuse, F-actin characteristic

of branched actin. Bundle density and F-actin content of bundled structures was low compared to those in networks containing dyn2, but no α-actinin **(Fig. S5B,C,D)**. α-Actinin was barely detectable along bundles; only faint punctate structures decorated some bundles **(Fig. S5A, upper panels)**. The low extent of bundling by 200 nM α-actinin in branched networks likely results from an impaired ability of branched filaments to align and crosslink as bundles.

Nonetheless, 460 nM dyn2 promoted formation of prominent F-actin bundles in branched networks in the absence and presence of 200 nM α-actinin **(Fig.S5A, lower panels, and Fig. S5B)**. In networks containing dyn2 and α-actinin, bundle density and F-actin content of bundles were increased compared to networks formed by 200 nM α-actinin alone, but decreased compared to networks containing only dyn2 **(Fig. S5C,D)**. Surprisingly, punctae of Alexa555-α-actinin decorated dyn2-dependent bundled structures predominately at sites near their ends or where bundles appeared to intersect **(Fig. S5A, lower panels)**. Since α-actinin crosslinks actin filaments as a meshwork under some conditions (Pelletier *et al.*, 2003; Lieleg *et al.*, 2010), the amount of α-actinin available to bind bundles could be limited by its associations with branched actin filaments in these networks. Alternatively, filaments in bundles formed by dyn2 and cortactin might be restricted in their ability to bind α-actinin due to steric constraints (Winkelman *et al.*, 2016) or by competition with either dyn2 or cortactin for actin binding sites along filaments.

Because branched actin antagonized filament bundling by α-actinin, to determine if α-actinin is targeted to dyn2-dependent bundles, we generated networks under conditions where the extent of filament branching was low **(Fig. 6, Video6a)**. Cortactin

is a weak NPF and branching density in networks generated by Arp2/3 complex and cortactin is lower than in networks generated by Arp2/3 complex and the synergistic activities of GST-VCA and cortactin (Weaver *et al.*, 2001; Helgeson and Nolen, 2013). Under conditions of low branch density, 200 nM α-actinin alone bundled filaments amidst a background of diffuse, unstructured F-actin **(Fig. 6A,C,D)**. Individual bundled structures accumulated Alexa555-α-actinin over time, even after F-actin accumulation had plateaued **(Fig. 6E, F)**. Consistently, the ratio of α-actinin fluorescence to phalloidin fluorescence along individual bundles also increased over time **(Fig. 6G, Video6b)**. Thus, when branch density is low, some filaments in Arp2/3 complex-dependent networks are bundled by 200 nM α-actinin.

As expected, the bundled structures formed in reactions containing 400 nM dyn2 and 200 nM α-actinin (with GTP) were more abundant and contained more F-actin compared to those formed by 200 nM α-actinin alone **(Fig. 6A-E)**. Although Alexa555-α-actinin associated with dyn2-dependent bundles over time **(Fig. 6B,F)**, the ratio of Alexa555-α-actinin:F-actin fluorescence was low compared to that for bundles formed by α-actinin alone **(Fig. 6G)**. Interestingly, bright Alexa-555-α-actinin-positive punctae were observed within 1-2 min in reactions containing dyn2 and GTP and remained particularly enriched at sites where bundled structures appeared to interconnect **(Fig. 6B, Video6a)**. Bundled structures formed in reactions in which GMPPCP was substituted for GTP **(Fig. S6)** contained slightly less F-actin, less α-actinin and a lower ratio of Alexa555-α-actinin:phalloidin fluorescence than bundles formed in reactions containing GTP **(Fig. 6E-G, Fig. S6)**. These data show that dyn2 promotes robust filament bundling but binding of α-actinin to bundled structures is limited relative to its

binding to bundles formed by α-actinin alone. Compared to networks containing GMPPCP, the presence of GTP in bundled networks formed by dyn2 increased the rate at which α-actinin associated with individual bundles. The decreased association of α-actinin to dyn2-dependent actin bundled structures is consistent with data obtained from cellular experiments in which the spatial distribution and amount of α-actinin associated with lamellipodial and lamellar F-actin networks increased in U2-OS cells when cellular [dyn2] was decreased using dyn2-specific siRNAs (Mooren *et al.*, 2009; Menon *et al.*, 2014). Taken together, these data show that dyn2 and cortactin antagonize branched actin nucleation in favor of filament bundling within Arp2/3 complex-dependent actin networks. Moreover, bundled structures generated by dyn2 and cortactin are restricted in binding α-actinin via a process that is regulated by GTP hydrolysis.

Discussion

Our findings support three conclusions about the mechanism by which dyn2 specifies actin filament organization within branched actin networks. First, dyn2 promotes filament bundling within reconstituted branched networks by decreasing branched actin nucleation by Arp2/3 complex. Second, dyn2 and cortactin crosslink actin filaments as bundles. Third, dyn2 GTPase activity modulates the sub-structure of filament bundles to regulate bundle expansion and the association of actin binding proteins. These activities support a hypothesis that dyn2, with cortactin, tunes the architecture of branched actin networks to promote assembly of actomyosin and other F-actin structures (Chua *et al.*, 2009; Mooren *et al.*, 2009; Menon *et al.*, 2014).

It is generally assumed that Arp2/3 complex generates sheet-like arrays of branched and interconnected filaments (reviewed in Blanchoin et al., 2014; Wu et al., 2012). However, filaments nucleated by Arp2/3 complex give rise to actin networks of varied architectures: Ena-VASP proteins protect from capping and elongate filaments generated by Arp2/3 complex to form uniformly-oriented bundled filaments of filopodia (Svitkina *et al.*, 2003); α-actinin and non-muscle myosin II associate with Arp2/3 complex-dependent actin filaments to generate transverse actomyosin arcs of lamella (Hotulainen and Lappalainen, 2006; Burnette *et al.*, 2011; Michael *et al.*, 2016); and Arp2/3 complex and *Listeria* ActA nucleate branched actin filaments on the surface of bacteria, yet bundled filaments predominate in comet tails formed by *Listeria in vivo* (Jasnin *et al.*, 2013). Based on their localizations within these and other Arp2/3 complex dependent networks, investigating a role for dyn2 and cortactin in organizing network morphology is warranted (Lee and De Camilli, 2002; Ferguson *et al.*, 2009; Anantharam *et al.*, 2011; Destaing *et al.*, 2013; Leikina *et al.*, 2013; Menon *et al.*, 2014; Palmer *et al.*, 2015).

It is challenging, but necessary, to separate the endocytic and actin regulatory functions of dynamins. Evidence supporting a direct role for dyn2 in regulating actin networks exists. Expressed mutant dynamin2 proteins that function in endocytosis did not restore cytoskeletal networks in dyn2-depleted cells (Menon *et al.*, 2014). Additionally, F-actin binding by the dynamin homolog, Vps1, supports endocytosis in budding yeast (Palmer *et al.*, 2015) and both branched and bundled actin filaments are required for endocytosis in fission yeast (Skau *et al.*, 2011). Although dyn2 is not required for Arp2/3 complex-dependent movement of intracellular bacteria, dyn2

influenced the dynamics, morphology and rate of motility of actin tails formed by *Listeria monocytogenes* in cells, a process that does not involve endocytosis once bacteria have entered the cytoplasm (Lee and De Camilli, 2002); cortactin was also implicated in actin tail-mediated *Listeria* invasion between cells (Barroso *et al.*, 2006). Hence, filament bundling by dyn2 and cortactin could optimize actin tail structure for efficient cell-to-cell spread (Henmi *et al.*, 2011).

Dyn2 promotes filament bundling by inhibiting actin nucleation and, with cortactin, crosslinking actin filaments

To bundle, actin filaments must diffuse, align and bind a threshold concentration of a filament crosslinking protein (Lieleg *et al.*, 2010). The morphology of crosslinked actin networks formed *in vitro* also depends on the competing processes of filament assembly and entanglement, which restrict filament mobility and alignment as filaments become long (Falzone *et al.*, 2012). By inhibiting branched nucleation, dyn2 promotes formation of unbranched filaments that, at early times in the reactions, can diffuse and align. In reconstituted networks containing dyn2 and cortactin, the earliest F-actin structures detected appeared as small, brightly-stained bundles. Subsequently, the overall morphology of bundled networks was established and continued actin assembly within existing bundles expanded the bundles.

Surprisingly, nascent bundled structures were not observed at early times in reactions observed using TIRF microscopy where filament diffusion is restricted by the closely-apposed chamber surface. Rather, filament bundles formed as a result of collisions of elongating filaments followed by continued elongation along the

interacting filaments. Colliding filaments often acutely changed direction to align and elongate other filaments to propagate as bundles. Hence, bundled structures viewed using TIRF microscopy expanded as a consequence of filament elongation. In some cases, *de novo* nucleation generated bundled filaments when newly nucleated filaments elongated along a mother filament without forming an apparent branched junction. Together, our observations are consistent with a model in which dyn2 and cortactin antagonize branched nucleation activity to form an F-actin structure that specifies bundling of unbranched filaments. Because filaments observed using TIRF are restricted in diffusion due to proximity to the sample chamber surface, we cannot rule out that bundling results from direct remodeling filaments at Arp2/3 complex-dependent junctions into crosslinked filaments, but observations under different conditions revealed no such events.

Although dynamin isoforms (Gu *et al.*, 2010; Palmer *et al.*, 2015) and dynamin-related proteins (Hatch *et al.*, 2016) are reported to directly bundle actin filaments as detected by low-speed sedimentation *in vitro*, dyn2 was not sufficient to generate bundles in reconstituted networks. As predicted from other sedimentation experiments (Mooren *et al.*, 2009; Yamada *et al.*, 2013) interactions of dyn2 and cortactin were required for robust filament bundling. Dyn2, which exists as tetramers and higher-order oligomers (Ramachandran *et al.*, 2007), could bind several molecules of cortactin, creating a scaffold that crosslinks several actin filaments via interactions with the fourth F-actin binding repeat of each cortactin molecule (Weed *et al.*, 2000; Schafer *et al.*, 2002; Mooren *et al.*, 2009; Yamada *et al.*, 2013). Recently, an alternate mechanism for cortactin-mediated actin filament crosslinking was proposed in which single cortactin

molecules crosslink filaments via interactions of different sets of F-actin-binding repeat sequences within the N-terminal half of a single cortactin molecule with aligned, paired actin filaments (Helgeson *et al.*, 2014). However, F-actin bundles were not observed in reconstituted networks unless both dyn2 and cortactin were present, thus, regardless of how cortactin binds actin filaments, a complex of dyn2 and cortactin is required for robust bundling *in vitro*. An intriguing possibility is that oligomeric dyn2 aligns filaments for efficient crosslinking by cortactin's F-actin-binding repeats through direct interactions of actin filaments with the F-actin binding regions of dyn2 stalks (Gu *et al.*, 2010). In sum, we speculate that a complex of dyn2 and cortactin bind and concomitantly crosslink actin filaments to form a "bundle template", a collection of crosslinked filaments primed to elongate and propagate assembly of bundled actin filaments.

GTP hydrolysis by dyn2 regulates bundle structure and crosslinking by α-actinin

GTP was not required for filament bundling, but GTP influenced the overall morphology of bundled networks and the rate at which α-actinin associated with dyn2-dependent bundles. In the presence of GTP, bundled structures were long and interconnected. With non-hydrolyzable GTP (or without guanine nucleotide), bundled networks were compact, isolated and loosely connected. Consistently, the fraction of 2-filament bundles observed using TIRF microscopy increased steadily in the presence of GTP, indicating persistent bundling over time compared to bundling in the presence of non-hydrolyzable GTP. These effects of dyn2 GTPase activity on dyn2-dependent bundles are consistent with our previous findings that the packing of filaments within

actin bundles pre-assembled *in vitro* by dyn2 and cortactin increased upon addition of GTP to the bundles (Mooren *et al.*, 2009). Finally, dyn2-dependent bundles gradually accumulate Alexa555-α-actinin in a manner that is enhanced by GTP. We conclude that GTP hydrolysis-dependent conformational changes within dyn2 molecules, possibly linked with its disassembly, regulates bundle expansion.

Recent observations suggest that sorting actin filament crosslinkers to specific F-actin networks depends, in part, on the geometric spacing of filaments (Winkelman *et al.*, 2016). Because dyn2 influenced the spatial distribution of α-actinin in branched actin networks in living cells, we asked if dyn2-dependent bundles bound α-actinin. Although dyn2-dependent bundles bind α-actinin, the ratio of α-actinin:F-actin is low compared to bundles formed by α-actinin alone, suggesting that dyn2 and cortactin specify a bundle architecture that restricts binding of α-actinin. This result is consistent with observations in U2-OS cells where the spatial distribution of α-actinin within lamellipodial networks, and in the actin cytoskeleton as a whole, increased when cellular [dyn2] was decreased (Mooren *et al.*, 2009; Menon *et al.*, 2014). Loss of dyn2-dependent bundling in lamellipodia of dyn2-depleted cells could yield branched actin filaments that are stabilized by α-actinin or other crosslinkers as a branched meshwork. Together, our results support a model in which dyn2 specifies a bundled filament architecture and regulates both bundle expansion and crosslinking by α-actinin in a GTPase-dependent manner.

During formation of nascent actomyosin at the edge of migrating cells, bundled F-actin and myosin II assemblies are proposed to coalesce near the leading membrane and assemble as transverse arcs near the lamellipod-lamellum boundary as they flow

rearward (Beach *et al.,* 2017; Burnette *et al.,* 2011; Fenix *et al.,* 2016; Hotulainen and Lappalainen, 2006; Hu *et al.,* 2017). In U2-OS cells, dyn2 is enriched at the leading edge of lamellipodial protrusions where it is implicated to support formation of actomyosin (Menon *et al.*, 2014). We show that dyn2 and cortactin promote formation of mixed-polarity bundles, characteristic of the organization of non-muscle actomyosin (Cramer, 1999). We speculate that bundled structures initiated by dyn2 and cortactin may arise as a result of filament overlap along the edge of protruding membrane extensions; subsequent association of bundled filaments with nascent myosin II assemblies generate nascent actomyosin. Whether dyn2 specifies a filament architecture ideally suited for co-assembly with myosin II filaments remains to be investigated.

Dyn2-dependent bundling could locally tune filament architectures in other F-actin networks. A dyn2-cortactin complex is proposed to organize and stabilize uniformly-oriented bundled filaments in filopodia of neurons and H1299 cells (Yamada *et al.*, 2013, 2016) and dyn2 has been implicated in organizing actin filaments in podosomes, invadopodia and finger-like protrusions enriched at sites of cell-cell fusion (Ochoa *et al.*, 2000; Baldassarre *et al.*, 2003; Bruzzaniti *et al.*, 2005; Sens *et al.*, 2010; Destaing *et al.*, 2013; Shin *et al.*, 2014). An endocytic function for dyn2 in processes associated with some of these actin-rich protrusions is not ruled out, but endocytic and actin functions executed by dynamin2 may also be linked, making it challenging to separate these functional roles (Taylor *et al.*, 2012; Grassart *et al.*, 2014; Palmer *et al.*, 2015). Altogether, our results support a role for dyn2 in locally tuning actin filament architecture to selectively give rise to actin structures required for specialized functions.

Acknowledgements

Material and methods

Proteins and reagents

Actin was purified from acetone powder of rabbit muscle (Pel-Freez Biologicals, AR) and gel-filtered on Sephadex G-200 (Spudich and Watt, 1971). Pyrenyl-actin (Bryan and Coluccio, 1985) was prepared using N-(1-pyrene) iodoacetamide (Invitrogen, MA). Arp2/3 complex was purified from bovine calf thymus (Higgs *et al.*, 1999). Recombinant glutathione *S*-transferase (GST)-cortactin and GST-cortactin-W525K were expressed in bacteria and purified as described (Mooren *et al.*, 2009). GST was removed from each protein by cleavage with TEV-protease (Invitrogen). His-tagged rat dyn2 was expressed in baculovirus-infected Hi5 insect cells and purified using Talon affinity resin (Mooren et al., 2009; Lin et al., 1997). A fusion protein of GST and the C-terminal region of human N-WASp (GST-VCA) (Egile *et al.*, 1999) was expressed in *E. coli* and purified by affinity on glutathione-agarose. His-tagged human α-actinin-4 was expressed in *E. coli* and purified using Talon affinity resin and chromatography on a MonoQ column (Winkelman et al., 2016); the plasmid for bacterial expression of α-actinin-4 was a gift from David Kovar (University of Chicago). Alexa555-α-actinin-4 was prepared by reacting a 5-fold molar excess of Alexa555-maleimide (Thermo Fisher Scientific) in DMSO with α-actinin-4 dialyzed in 20mM Tris-HCl, pH 8.0, 100mM NaCl, 0.2 mM EDTA, 0.01% NaN_3, and 10% glycerol. GTP, GMPPNP and GMPPCP were purchased from Sigma Aldrich. Alexa647-phalloidin was purchased from Invitrogen.

Purified proteins were dialyzed in the following buffers before use: actin in G buffer (2

mM Tris-HCl, pH 8.0, 0.2 mM ATP, 0.1 mM dithiothreitol (DTT), 0.005% NaN_3, and

0.2 mM $CaCl_2$); Arp2/3 complex, GST-VCA, cortactin and cortactin-W525K in 20 mM

Tris-HCl, pH 8.0, 50 mM KCl, 1 mM EDTA, 0.2 mM EGTA, 0.5 mM DTT, and 0.1

mM ATP; dyn2 in 20 mM HEPES, pH 7.5, 150 mM KCl, 1 mM EDTA, 1 mM EGTA,

0.5 mM DTT; α-actinin-4 and Alexa555-α-actinin-4 in 20 mM Tris-HCl, pH 8.0, 10%

glycerol, 100 mM NaCl, 0.2 mM EDTA, 1mM DTT, and 0.01% NaN_3.

Proteins were quantified from absorbance at 280 nm (290 nm for actin) using the

following molar extinction coefficients: actin, 26,600 M^{-1} cm^{-1}; dyn2, 53,490 M^{-1} cm^{-1};

Arp2/3 complex, 224,000 M^{-1} cm^{-1}; cortactin, 69,060 M^{-1} cm^{-1}; cortactin-W525K,

67,855 M^{-1} cm^{-1}; GST-VCA, 46,970 M^{-1} cm^{-1}; α-actinin-4, 124,000 M^{-1} cm^{-1} for a

monomer (α-actinin-4 concentrations indicate the concentration of the dimeric protein).

Visualizing and analysis of reconstituted F-actin networks

Glass coverslips (No. 1.5) and microscope slides were cleaned in acetone and 1M KOH,

treated with 1% (3-aminopropyl)triethoxysilane (Sigma Aldrich) and passivated with 30

mg/ml methoxy-PEG succinimidyl succinate, MW 5000 (JenKem, TX) (Helgeson and

Nolen, 2013). Reaction chambers were assembled from passivated coverslips attached

to glass slides with strips of double-sided tape spaced 3-4 mm apart to create ~10 μl

channels. Actin networks were reconstituted from 2.5 μM actin, 50 nM Arp2/3

complex, 2 nM GST-VCA, and 400 nM cortactin in a buffer containing 20 mM

imidazole, pH 7.0, 50 mM KCl, 1 mM EGTA, 5 mM $MgCl_2$, 5 mg/ml glucose, 0.1

mg/ml glucose oxidase, 20 mg/ml catalase, 0.5% β-mercaptoethanol, 2 mM Tris-HCl,

pH 8.0, 0.2 mM ATP, and 250 nM Alexa647-phalloidin; reactions also contained either 1.5 mM GTP or 1.5 mM GMPPCP and varying concentrations of dyn2. Alexa555-α-actinin-4 was included at 100 nM or 200 nM as indicated. Each reaction was mixed, loaded into a chamber, sealed with molten Valap (1:1:1 mixture of Vaseline, lanolin, and paraffin wax, by weight), and immediately transferred to the microscope stage for imaging. Imaging was performed on a Nikon Eclipse Ti microscope equipped with a CSU-X1 spinning disk (Yokogawa), a 60X 1.4 numerical aperture (N.A.) oil objective lens, lasers for excitation at 488 nm, 561 nm and 647 nm, and an ORCA-Flash4.0 digital CMOS camera (Hamamatsu, Japan). Timelapse images were collected at 1 min intervals for 30-45 min. A z-stack of 20 images (0.8 μm step/image and 400 ms exposure/image) was acquired at each timepoint. Image collection began at least 20 μm away from the coverslip surface to minimize surface effects. In reactions containing Alexa647-phalloidin and Alexa555-α-actinin-4, images were collected at 561 nm and 647 nm from each image of the stack before advancing in the z-dimension. Each z-stack was rendered as a 2D-maximal intensity projection using tools available in ImageJ (NIH). Images were further processed in ImageJ for background subtraction by subtracting the first frame of each timelapse sequence from all others in the movie.

The extent of bundling in reconstituted networks was quantified using a metric called "Bundle density" which is defined as the number of maximal intensity peaks of Alexa647-phalloidin fluorescence per micron along 5-pixel wide line scans oriented in the x and y directions of each image; in total, line scans covered 1.9 mm/image at each time point (see Fig. S1 in Supplemental Data). A MATLAB (MathWorks, MA)

algorithm was used to identify local fluorescence intensity maxima along line scans; an intensity peak was scored as a bundle based on its prominence along the line relative to nearby peaks and an intensity higher than an empirically established threshold above background. Because reconstituted networks of different composition were compared within each experiment (i.e., a dyn2 dose-response), the bundle density in each network at each timepoint is reported. Independent network experiments were repeated at least three times, except where noted in the figure legend. The MATLAB code for identification of local maximal intensites is available on request.

Pyrenyl-actin polymerization assay

Actin polymerization in solution was measured from the fluorescence of pyrenyl-actin (Bryan and Coluccio, 1985) using excitation at 365 nm and emission at 386 nm. Unless otherwise indicated, reactions contained 1.5 μM actin (10% pyrene-labeled), 20 nM Arp2/3 complex, 5 nM GST-VCA, 400 nM cortactin, 1.5 mM GTP or GMPPNP, and varying concentrations of dyn2 in 20 mM imidazole, pH 7.0, 2 mM Tris-HCl, pH 8.0, 50 mM KCl, 1 mM EGTA, 2 mM $MgCl_2$, 0.2 mM ATP, and 0.1 mM DTT. Assays to determine the critical concentration for actin assembly were performed as described (Kouyama and Mihashi, 1981).

Total internal reflection fluorescence (TIRF) microscopy and image analysis

TIRF microscopy (TIRF-M) was used to quantify branched nucleation by Arp2/3 complex and to observe filament bundling. To quantify filament branching, glass coverslips and slides were cleaned in 2% Hellmanex (Sigma Aldrich, MO), rinsed in

water, incubated sequentially in 1 M KOH and 1 M HCl and coated with 14 nM of N-ethylmaleimide-modified skeletal muscle myosin prepared as described (Veigel *et al.*, 1998) and rinsed with 1% BSA. Reactions contained 1.5 µM actin (30% Alexa 488-labeled), 20 nM Arp2/3, 3 nM GST-VCA, with and without 200 nM cortactin, with and without 200 nM dyn2, 0.4 mM ATP, and either 1.5 mM GTP or 1.5 mM GMP-PNP in a buffer containing 50 mM KCl, 1 mM $MgCl_2$, 1 mM EGTA, 10 mM imidazole, pH 7.0, 0.5% methylcellulose, 30 mM glucose, 200 mM DTT, 40 µg/ml catalase, 0.2 µg/ml glucose oxidase. TIRF microscopy was performed on an Olympus X71 inverted microscope equipped with a 60X, 1.45 N.A. oil objective lens, an Argon laser and an ORCA-Flash4.0 CMOS camera (Hamamatsu, Japan). Images (100 ms exposure) were collected at 1-s interval over 10 min using MetaMorph software (Molecular Devices, CA). Branching density was quantified from the timelapse images by counting the number of branches per "mother" filament length.

To observe interactions of filaments and filament bundling using TIRF-M, sample chambers comprised of passivated PEG-treated coverslips and slides were prepared as described for the network assays. Reactions contained 1 µM actin (30% Alexa 488 labeled), 50 nM Arp2/3 complex, 2 nM GST-VCA, 400 nM cortactin (or 400 nM cortactin-W525K), 400 nM dyn2, 0.2 mM ATP, 1.5 mM GTP (or 1.5 mM GMPPCP) in a buffer containing 20 mM imidazole, pH 7.0, 75 mM KCl, 1 mM EGTA, 5 mM $MgCl_2$, 0.3% methylcellulose, 40 mM DTT, 25 mM glucose, 0.1 mg/ml glucose oxidase, and 20 µg/ml catalase. To obtain a population of single actin filaments that elongated and interacted soon after the start of imaging, reactions were incubated for 2-

3 min prior to delivery into the sample chamber. Images were collected at a rate of 1 frame/4 s for 0.5 s.

Timelapse images were processed in ImageJ by background subtraction with a rolling ball radius of 10 pixels and blurred using a Gaussian filer of radius 0.6 pixel. Filament tracking events are defined as events in which one actin filament elongated in close association with another filament, forming a 2-(or more)- filament bundle. The duration of tracking events was determined by manually recording the start time and end time of filament tracking for each event. Filament tracking events were scored as parallel if the bundled filaments were oriented with barbed ends in the same orientation, or anti-parallel if the bundled filaments were oppositely oriented. All tracking events detected in the 1024 x 1024-pixel field of each timelapse sequence were scored.

The fraction of bundled filaments formed over time in reactions was quantified from timelapse movies by first applying a minimal intensity threshold that revealed all F-actin structures in the field. The area corresponding to all actin filaments in the thresholded image was determined at each timepoint using measurement tools in ImageJ; this value estimated the amount of F-actin in each region of interest. A second intensity threshold was subsequently applied that revealed only F-actin structures composed of 2 or more filaments. The fractional area of bundled structures was determined from the ratio of the areas of 2-or more-filament structures/ all filament structures. Multiple non-overlapping regions of interest were analyzed for each reaction.

Statistical analysis

GraphPad Prism software was used for all statistical analyses. Quantitative data are expressed as mean±standard error of the mean (mean±SEM) indicated by error bars. A two-tailed Student's *t*-test was used for comparisons between two groups, with statistical significance indicated by a *p*-value. For multiple comparisons, a one-way analysis of variance (ANOVA) with Tukey's comparison of individual pairs of samples was performed. Experiments were performed three times, unless noted in the legend.

References

Anand, R., Eschenburg, S., and Reubold, T. F. (2016). Crystal structure of the GTPase domain and the bundle signalling element of dynamin in the GDP state. Biochem. Biophys. Res. Commun. *469*, 76–80.

Anantharam, A., Bittner, M. A., Aikman, R. L., Stuenkel, E. L., Schmid, S. L., Axelrod, D., and Holz, R. W. (2011). A new role for the dynamin GTPase in the regulation of fusion pore expansion. Mol. Biol. Cell *22*, 1907–1918.

Baldassarre, M., Pompeo, A., Beznoussenko, G., Castaldi, C., Cortellino, S., McNiven, M. A., Luini, A., and Buccione, R. (2003). Dynamin Participates in Focal Extracellular Matrix Degradation by Invasive Cells. Mol. Biol. Cell *14*, 1074–1084.

Beach, J. R., Bruun, K.S., Shao, L., Li, D., Swider, Z., Remmert, K., Zhang, Y., Conti, M.A., Adelstein, R.S., Rusan, N.M., et al. (2017). Actin dynamics and competition for myosin monomer govern the sequential amplification of myosin filaments. Nat. Cell Biol. *19*, 85–93.

Blanchoin, L., Boujemaa-Paterski, R., Sykes, C., and Plastino, J. (2014). Actin dynamics, architecture, and mechanics in cell motility. Physiol. Rev. *94*, 235–263.

Bruzzaniti, A., Neff, L., Sanjay, A., Horne, W. C., Camilli, P. De, and Baron, R. (2005). Dynamin Forms a Src Kinase – sensitive Complex with Cbl and Regulates Podosomes and Osteoclast Activity. *16*, 3301–3313.

Bryan, J., and Coluccio, L. M. (1985). Kinetic analysis of f-actin depolymerization in the presence of platelet gelsolin and gelsolin-actin complexes. J. Cell Biol. *101*, 1236–1244.

Burke, T. A., Christensen, J. R., Barone, E., Suarez, C., Sirotkin, V., and Kovar, D. R. (2014). Homeostatic actin cytoskeleton networks are regulated by assembly factor competition for monomers. Curr. Biol. *24*, 579–585.

Burnette, D. T., Manley, S., Sengupta, P., Sougrat, R., Davidson, M. W., Kachar, B., and Lippincott-Schwartz, J. (2011). A role for actin arcs in the leading-edge advance of migrating cells. Nat. Cell Biol. *13*, 371–381.

Chappie, J. S., Mears, J. A., Fang, S., Leonard, M., Schmid, S. L., Milligan, R. A., Hinshaw, J. E., and Dyda, F. (2011). A pseudoatomic model of the dynamin polymer identifies a hydrolysis-dependent powerstroke. Cell *147*, 209–222.

Chhabra, E. S., and Higgs, H. N. (2007). The many faces of actin: matching assembly factors with cellular structures. Nat. Cell Biol. *9*, 1110–1121.

Chua, J., Rikhy, R. and Lippincott-Schwartz, J. (2009). Dynamin 2 orchestrates the global actomyosin cytoskeleton for epithelial maintenance and apical constriction. Proc. Natl. Acad. Sci. *106*, 20770–20775.

Cramer, L. P. (1999). Organization and polarity of actin filament networks in cells: implications for the mechanism of myosin-based cell motility. Biochem. Soc. Symp. *65*, 173–205.

Destaing, O., Ferguson, S. M., Grichine, A., Oddou, C., De Camilli, P., Albiges-Rizo, C., and Baron, R. (2013). Essential Function of Dynamin in the Invasive Properties and Actin Architecture of v-Src Induced Podosomes/Invadosomes. PLoS One *8*, e77956.

Egile, C., Loisel, T. P., Laurent, V., Li, R., Pantaloni, D., Sansonetti, P. J., and Carlier, M. F. (1999). Activation of the CDC42 effector N-WASP by the Shigella flexneri IcsA protein promotes actin nucleation by Arp2/3 complex and bacterial actin-based motility. J. Cell Biol. *146*, 1319–1332.

Falzone, T. T., Lenz, M., Kovar, D. R., and Gardel, M. L. (2012). Assembly kinetics detemine the architecture of α -actinin crosslinked F-actin networks. Nat. Commun. *3*, 861–869.

Fenix, A. M., Taneja, N., Buttler, C. A., Lewis, J., Van Engelenburg, S. B., Ohi, R., and Burnette, D. T. (2016). Expansion and concatenation of nonmuscle myosin IIA filaments drive cellular contractile system formation during interphase and mitosis. Mol. Biol. Cell *27*, 1465–1478.

Ferguson, S., Raimondi, A., Paradise, S., Shen, H., Mesaki, K., Ferguson, A., Destaing, O. Ko, G., Takasaki, J., Cremona, O. *et al.* (2009). Coordinated Actions of Actin and BAR Proteins Upstream of Dynamin at Endocytic Clathrin-Coated Pits. Dev. Cell *17*, 811–822.

Grassart, A., Cheng, A. T., Hong, S. H., Zhang, F., Zenzer, N., Feng, Y., Briner, D. M., Davis, G. D., Malkov, D., and Drubin, D. G. (2014). Actin and dynamin2 dynamics and interplay during clathrin-mediated endocytosis. J. Cell Biol. *205*, 721–735.

Gu, C., Yaddanapudi, S., Weins, A., Osborn, T., Reiser, J., Pollak, M., Hartwig, J., and Sever, S. (2010). Direct dynamin-actin interactions regulate the actin cytoskeleton. EMBO J. *29*, 3593–3606.

Hatch, A. L., Ji, W.-K., Merrill, R. A., Strack, S., and Higgs, H. N. (2016). Actin filaments as dynamic reservoirs for Drp1 recruitment. Mol. Biol. Cell *27*, 3109–3121.

Helgeson, L. A., Prendergast, J. G., Wagner, A. R., Rodnick-smith, M., Nolen, B. J. (2014). Interactions with Actin Monomers , Actin Filaments , and Arp2 / 3 Complex Define the Roles of WASP Family Proteins and Cortactin in Coordinately Regulating Branched Actin. J. Biol. Chem. *289*, 28856-28869

Helgeson, L. A., and Nolen, B. J. (2013). Mechanism of synergistic activation of Arp2/3 complex by cortactin and N-WASP. eLife *2*, e00884.

Henmi, Y., Tanabe, K., and Takei, K. (2011). Disruption of microtubule network rescues aberrant actin comets in dynamin2-depleted cells. PLoS One *6*.

Higgs, H. N., Blanchoin, L., and Pollard, T. D. (1999). Influence of the C terminus of Wiskott-Aldrich syndrome protein (WASp) and the Arp2/3 complex on actin polymerization. Biochemistry *38*, 15212–15222.

Hinshaw, J. E. (2000). Dynamin and its role in membrane fission. Annu. Rev. Cell Dev. Biol. *16*, 483–519.

Hotulainen, P., and Lappalainen, P. (2006). Stress fibers are generated by two distinct actin assembly mechanisms in motile cells. J. Cell Biol. *173*, 383–394.

Hu, S., Dasbiswas, K., Guo, Z., Tee, Y. H., Thiagarajan, V., Hersen, P., Chew, T. L., Safran, S. A., Zaidel-Bar, R., and Bershadsky, A. D. (2017). Long-range self-organization of cytoskeletal myosin II filament stacks. Nat. Cell Biol. *19*, 133–141.

Jasnin, M., Asano, S., Gouin, E., Hegerl, R., Plitzko, J. M., Villa, E., Cossart, P., and Baumeister, W. (2013). Three-dimensional architecture of actin filaments in Listeria monocytogenes comet tails. Proc. Natl. Acad. Sci. *110*, 20521–20526.

Kouyama, T., and Mihashi, K. (1981). Fluorimetry Study of N-(1-Pyrenyl)iodoacetamide-Labelled F-Actin. Eur. J. Biochem. *114*, 33–38.

Krueger, E. W., Orth, J. D., Cao, H., and McNiven, M. A. (2003). A dynamin-cortactin-Arp2/3 complex mediates actin reorganization in growth factor-stimulated cells. Mol. Biol. Cell *14*, 1085–1096.

Lee, E., and De Camilli, P. (2002). Dynamin at actin tails. Proc. Natl. Acad. *99*, 161–166.

Leikina, E., Melikov, K., Sanyal, S., Verma, S. K., Eun, B., Gebert, C., Pfeifer, K., Lizunov, V. A., Kozlov, M. M., and Chernomordik, L. V. (2013). Extracellular annexins and dynamin are important for sequential steps in myoblast fusion. J. Cell Biol. *200*, 109–123.

Lieleg, O., Claessens, M. M. A. E., and Bausch, A. R. (2010). Structure and

dynamics of cross-linked actin networks. Soft Matter *6*, 218–225.

Lin, H. C., Barylko, B., Achiriloaie, M., and Albanesi, J. P. (1997). Phosphatidylinositol (4,5)-bisphosphate-dependent activation of dynamins I and II lacking the proline/arginine-rich domains. J. Biol. Chem. *272*, 25999–26004.

Lomakin, A. J., Lee, K.-C. C., Han, S. J., Bui, D. A., Davidson, M., Mogilner, A., and Danuser, G. (2015). Competition for actin between two distinct F-actin networks defines a bistable switch for cell polarization. Nat. Cell Biol. *17*, 1435-1445.

Marks, B., Stowell, M. H. B., Vallis, Y., Mills, I. G., Gibson, A., Hopkins, C. R., and McMahon, H. T. (2001). GTPase activity of dynamin and resulting conformation change are essential for endocytosis. Nature *410*, 231–235.

McNiven, M. A., Kim, L., Krueger, E. W., Orth, J. D., Cao, H., and Wong, T. W. (2000). Regulated interactions between dynamin and the actin-binding protein cortactin modulate cell shape. J. Cell Biol. *151*, 187–198.

Menon, M., Askinazi, O. L., and Schafer, D. A. (2014). Dynamin2 organizes lamellipodial actin networks to orchestrate lamellar actomyosin. PLoS One *9*, e94330.

Michael, M., Meiring, J. C. M., Acharya, B. R., Matthews, D. R., Verma, S., Han, S. P., Hill, M. M., Parton, R. G., Gomez, G. A., and Yap, A. S. (2016). Coronin 1B Reorganizes the Architecture of F-Actin Networks for Contractility at Steady-State and Apoptotic Adherens Junctions. Dev. Cell *37*, 58–71.

Mooren, O., Kotova, T., Moore, A., and Schafer, D. (2009). Dynamin2 GTPase and cortactin remodel actin filaments. J. Biol. Chem. *284*, 23995–24005.

Ochoa, G. Slepnev, V.I., Neff, L., Ringstad, N., Takei, K., Daniell, L., Kim, W., Cao, H., Mcniven, M., Baron, R. *et al.* (2000). A Functional Link between Dynamin and the Actin Cytoskeleton at Podosomes. *150*, 377–389.

Orth, J. D., Krueger, E. W., Cao, H., and McNiven, M. a (2002). The large GTPase dynamin regulates actin comet formation and movement in living cells. Proc. Natl. Acad. Sci. U. S. A. *99*, 167–172.

Palmer, S. E., Smaczynska-de Rooij, I. I., Marklew, C. J., Allwood, E. G., Mishra, R., Johnson, S., Goldberg, M. W., and Ayscough, K. R. (2015). A Dynamin-Actin Interaction Is Required for Vesicle Scission during Endocytosis in Yeast. Curr. Biol. *25*, 868–878.

Pelletier, O., Pokidysheva, E., Hirst, L. S., Bouxsein, N., Li, Y., and Safinya, C. R. (2003). Structure of actin cross-linked with α-actinin: A network of bundles. Phys.

Rev. Lett. *91*, 3–6.

Ramachandran, R., Surka, M., Chappie, J. S., Fowler, D. M., Foss, T. R., Song, B. D., and Schmid, S. L. (2007). The dynamin middle domain is critical for tetramerization and higher-order self-assembly. EMBO J. *26*, 559–566.

Rotty, J. D., Wu, C., Haynes, E. M., Suarez, C., Winkelman, J. D., Johnson, H. E., Haugh, J. M., Kovar, D. R., and Bear, J. E. (2015). Profilin-1 Serves as a gatekeeper for actin assembly by Arp2/3-Dependent and - Independent pathways. Dev. Cell *32*, 54–67.

Schafer, D. A., Weed, S. A., Binns, D., Karginov, A. V., Parsons, J. T., and Cooper, J. A. (2002). Dynamin2 and cortactin regulate actin assembly and filament organization. Curr. Biol. *12*, 1852–1857.

Sens, K. L., Zhang, S., Jin, P., Duan, R., Zhang, G., Luo, F., Parachini, L., and Chen, E. H. (2010). An invasive podosome-like structure promotes fusion pore formation during myoblast fusion. J. Cell Biol. *191*, 1013–1027.

Shin, N.-Y., Choi, H., Neff, L., Wu, Y., Saito, H., Ferguson, S. M., De Camilli, P., and Baron, R. (2014). Dynamin and endocytosis are required for the fusion of osteoclasts and myoblasts. J. Cell Biol. *207*, 73–89.

Skau, C. T., Courson, D. S., Bestul, A. J., Winkelman, J. D., Rock, R. S., Sirotkin, V., and Kovar, D. R. (2011). Actin filament bundling by fimbrin is important for endocytosis, cytokinesis, and polarization in fission yeast. J. Biol. Chem. *286*, 26964–26977.

Spudich, J. A., and Watt, S. (1971). The regulation of rabbit skeletal muscle contraction. I. Biochemical studies of the interaction of the tropomyosin-troponin complex with actin and the proteolytic fragments of myosin. J. Biol. Chem. *246*, 4866–4871.

Suarez, C., and Kovar, D. R. (2016). Internetwork competition for monomers governs actin cytoskeleton organization. Nat. Rev. Mol. Cell Biol. *17*, 799–810.

Svitkina, T. M., Bulanova, E. A., Chaga, O. Y., Vignjevic, D. M., Kojima, S. ichiro, Vasiliev, J. M., and Borisy, G. G. (2003). Mechanism of filopodia initiation by reorganization of a dendritic network. J. Cell Biol. *160*, 409–421.

Taylor, M. J., Lampe, M., and Merrifield, C. J. (2012). A feedback loop between dynamin and actin recruitment during clathrin-mediated endocytosis. PLoS Biol. *10*. Veigel, C., Bartoo, M. L., White, D. C. S., Sparrow, J. C., and Molloy, J. E. (1998). The stiffness of rabbit skeletal actomyosin cross-bridges determined with an optical tweezers transducer. Biophys. J. *75*, 1424–1438.

Warnock, D. E., Hinshaw, J. E., and Schmid, S. L. (1996). Dynamin self-assembly stimulates its GTPase activity. J. Biol. Chem. *271*, 22310–22314.

Weaver, A. M., Karginov, A. V., Kinley, A. W., Weed, S. A., Li, Y., Parsons, J. T., and Cooper, J. A. (2001). Cortactin promotes and stabilizes Arp2/3-induced actin filament network formation. Curr. Biol. *11*, 370–374.

Weed, S. A., Karginov, A. V., Schafer, D. A., Weaver, A. M., Kinley, A. W., Cooper, J. A., and Parsons, J. T. (2000). Cortactin localization to sites of actin assembly in lamellipodia requires interactions with F-actin and the Arp2/3 complex. J. Cell Biol. *151*, 29–40.

Winkelman, J. D., Suarez, C., Hocky, G. M., Harker, A. J., Morganthaler, A. N., Christensen, J. R., Voth, G. A., Bartles, J. R., and Kovar, D. R. (2016). Fascin- and α-Actinin-Bundled Networks Contain Intrinsic Structural Features that Drive Protein Sorting. Curr. Biol. *26*, 2697–2706.

Wu, C., Asokan, S. B., Berginski, M. E., Haynes, E. M., Sharpless, N. E., Griffith, J. D., Gomez, S. M., and Bear, J. E. (2012). Arp2/3 is critical for lamellipodia and response to extracellular matrix cues but is dispensable for chemotaxis. Cell *148*, 973–987.

Wu, H., and Parsons, J. T. (1993). Cortactin, an 80/85-kilodalton pp60src substrate, is a filamentous actin-Binding protein enriched in the cell cortex. J. Cell Biol. *120*, 1417–1426.

Yamada, H. Abe, T., Satoh, A., Okazaki, N., Tago, S., Kobayashi, K., Yoshida, Y., Oda, Y., Watanabe, M., Tomizawa, K., *et al.* (2013). Stabilization of Actin Bundles by a Dynamin 1/Cortactin Ring Complex Is Necessary for Growth Cone Filopodia. J. Neurosci. *33*, 4514–4526.

Yamada, H., Kobayashi, K., Zhang, Y., Takeda, T., and Takei, K. (2016). Expression of a dynamin 2 mutant associated with Charcot-Marie-Tooth disease leads to aberrant actin dynamics and lamellipodia formation. Neurosci. Lett. *628*, 179–185.
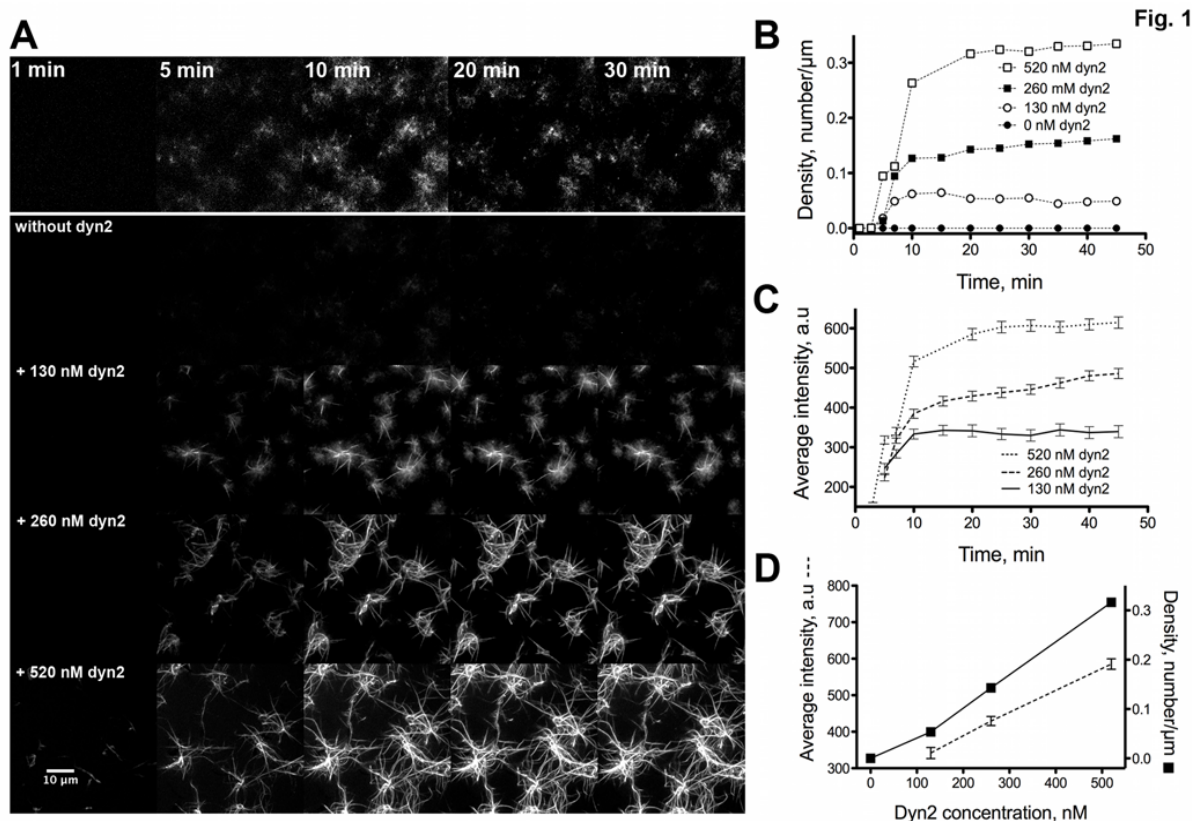
Figures

Figure 1. Dyn2 bundles actin filaments in reconstituted networks formed by Arp2/3 complex, GST-VCA, and cortactin.

Panel A. Timelapse images of F-actin networks reconstituted from 2.5 μM actin, 50 nM Arp2/3, 2 nM GST-VCA, 400 nM cortactin, 1.5 mM GTP and increasing concentrations of dyn2, as indicated, were collected using confocal microscopy. F-actin was detected by labeling with Alexa 647-phalloidin. The upper two rows show the same network formed in the absence of dyn2; enhanced gain was applied to highlight network features in images in the upper row; all other panels are displayed with identical gain settings. Data are representative of results from two independent experiments. The full timelapse sequences are shown in **Video1**.

Panel B. Plotted is bundle density over time for data from reactions shown in Panel **A**. Bundles were identified and bundle density quantified as described in 'Materials and Methods'. The total number of bundles was 118, 294, and 597 (at the 30 min timepoint) in reactions containing 130, 260, and 520 nM of dyn2, respectively.

Panel C. Plotted is the intensity of Alexa 647-phalloidin fluorescence of bundles (mean±SEM) over time.

Panel D. Plotted is bundle density and Alexa 647-phalloidin fluorescence of bundles (mean±SEM) vs. the concentration of dyn2 for the 20 min timepoint of reactions shown in Panel **A**.
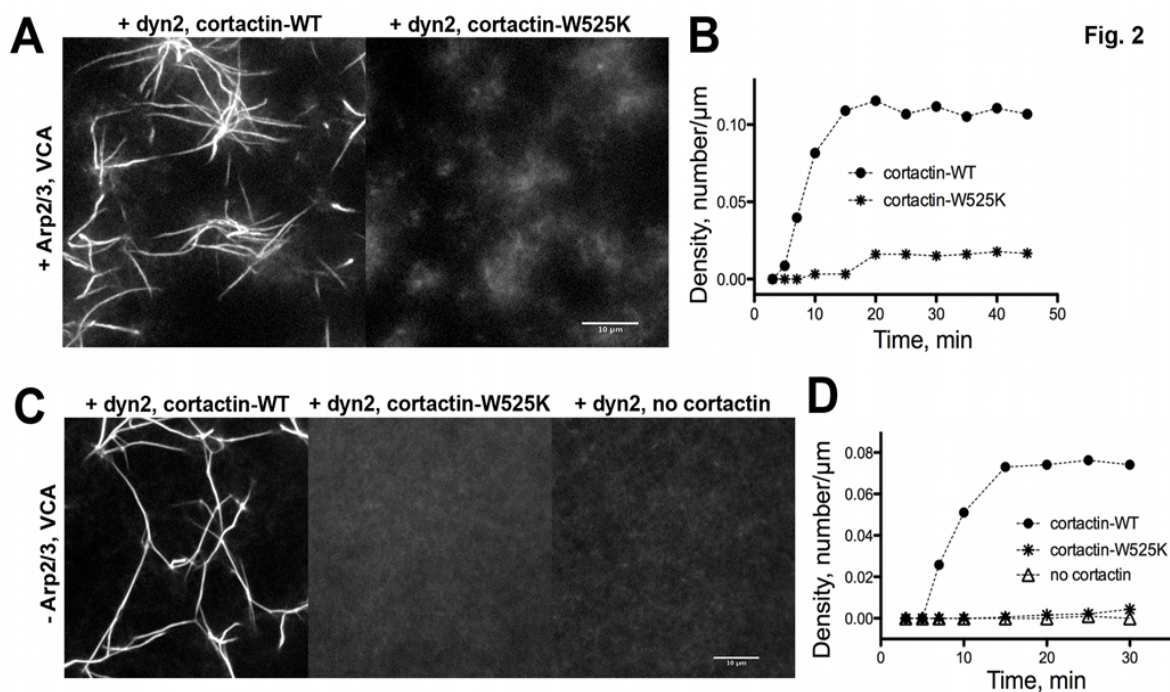
Figure 2. Interactions between dyn2 and cortactin are required for filament bundling in reconstituted actin networks generated with and without Arp2/3 complex.

Panel A. Confocal micrographs of reconstituted actin networks formed 20 min after mixing 2.5 μm actin, 50 nM Arp2/3 complex, 2 nM GST-VCA, 400 nM dyn2, and 1.5 mM GTP and either 400 nM of WT cortactin or mutant cortactin-W525K, as indicated. The timelapse sequence is shown in **Video2**.

Panel B. Plotted is bundle density over time for data from timelapse movies of reactions shown in Panel **A**. The total number of bundles analyzed was 215 and 30 (at 30 min timepoint), in reactions containing WT cortactin and cortactin-W525K, respectively.

Panel C. Confocal micrographs of reconstituted actin networks formed 20 min after mixing 2.5 μm actin, 400 nM dyn2, 1.5 mM GTP and with either 400 nM of WT cortactin, mutant cortactin-W525K or in the absence of cortactin. The timelapse sequence is shown in **Video3**.

Panel D. Plotted is bundle density over time for data from timelapse movies of reactions shown in Panel **C.** The total number of bundles analyzed was 138, 3, and 0 (at 20 min timepoint) in reactions containing WT cortactin, cortactin-W525K, or no cortactin, respectively.
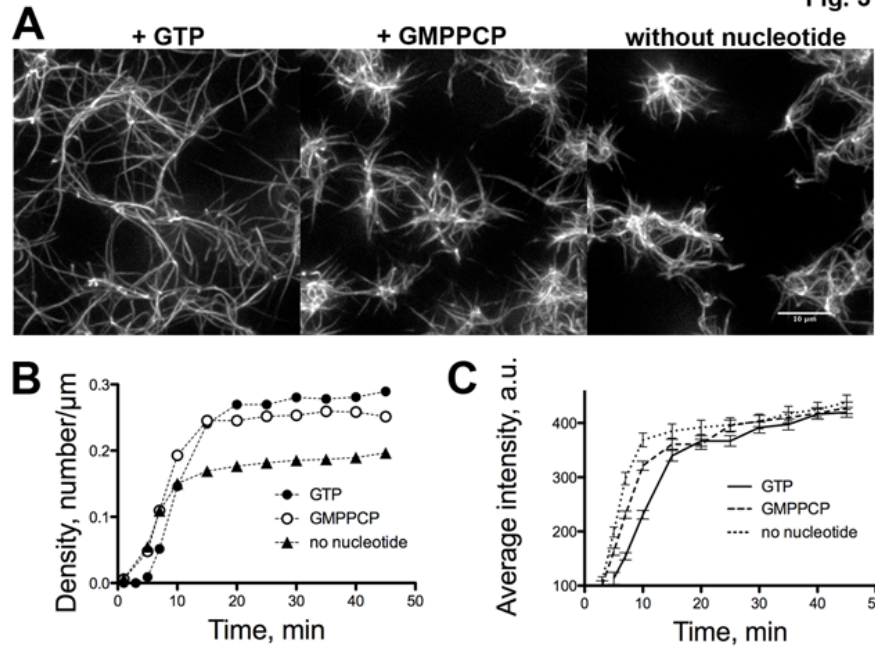
Fig. 3   77

Figure 3. Dyn2 GTPase activity regulates network morphology in reconstituted networks.

Panel A. Confocal micrographs of reconstituted networks formed 20 min in reactions containing 2.5 μM actin, 50 nM Arp2/3 complex, 2 nM GST-VCA, 400 nM cortactin, 400 nM dyn2 and either 1.5 mM GTP, GMPPCP, or without guanine nucleotide, as indicated. Timelapse sequences are shown in **Video4**.

Panel B. Plotted is bundle density over time for data from timelapse movies of reactions shown in Panel **A**. The total number of bundles analyzed was 502, 457, and 329 (at 20 min timepoint) in reactions containing GTP, GMPPCP, and no guanine nucleotide, respectively.

Panel C. Plotted is the average intensity of Alexa-647-phallidin in bundles (mean ± SEM) over time for data from timelapse movies of reactions shown in Panel **A**. Data are representative of results from three independent experiments.
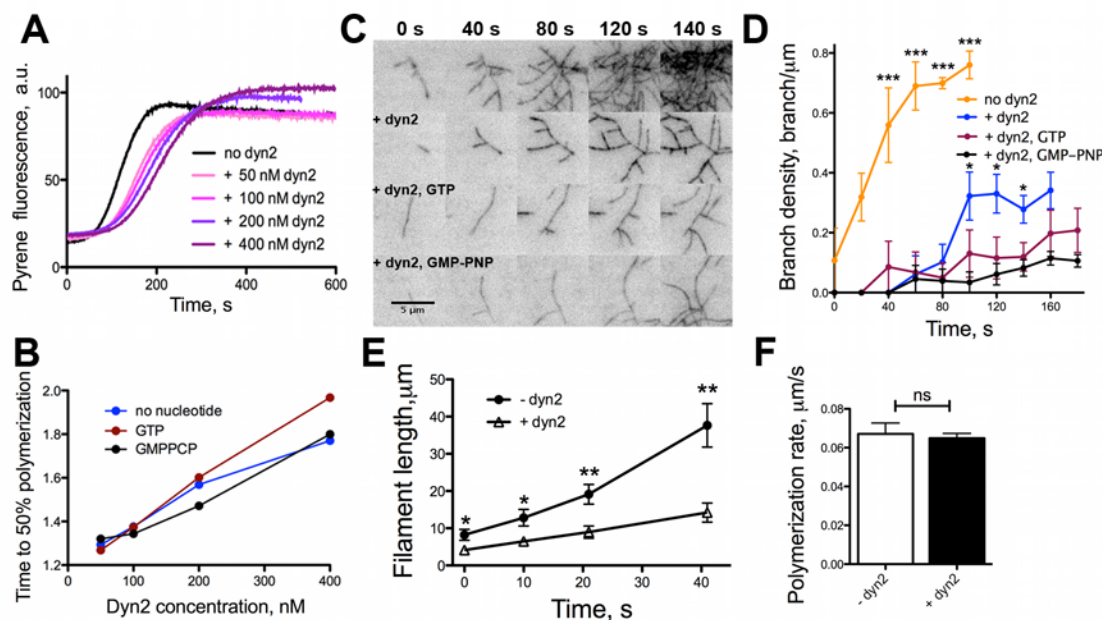
Figure 4. Dyn2 decreases actin nucleation and filament branching by Arp2/3 complex.

Panel A. Plotted is fluorescence of pyrenyl-actin over time in reactions containing 1.5 μM actin (10% pyrene-labeled), 20 nM Arp2/3, 5 nM GST-VCA, 200 nM cortactin and varying concentrations of dyn2, as indicated.

Panel B. Plotted is the time required to reach 50% polymerization as a function of increasing concentrations of dyn2; reactions are as described in panel A wth 1.5 mM GTP, GMP-PNP or without guanine nucleotide, as indicated. Data are normalized to the time required to achieve 50% polymerization in reactions without dyn2.

Panel C. Images show actin filaments observed using TIRF microscopy formed over time in reactions containing 1.5 μM actin (30% Alexa 488-labeled), 20 nM Arp2/3, 3 nM GST-VCA, 200 nM cortactin, with and without 200 nM dyn2 and with 1 mM GTP, GMP-PNP or without guanine nucleotide, as indicated.

Panel D. Plotted is branch density over time for data shown in Panel **C**. Data are presented as mean±SEM for three regions of interest from each acquisition period. One-way ANOVA was used to assess statistical significance among all samples between 40 and 100 s and, separately among all samples that contained dyn2 between 40 and 160 s. *p<0.05, ***p<0.001

Panel E. Plotted is total actin filament length assembled over time for reactions with and without 200 nM dyn2 shown in Panel **C**. Data are presented as mean±SEM (n=7 filaments for each condition). A two-tailed Student's *t*-test was used to assess significance; **p<0.01, ***p<0.001.

Panel F. Plotted is rate of filament elongation over time for filaments in movies shown in Panel **C**. Data are presented as mean±SEM (n=6 filaments for each condition). A two-tailed Student's *t*-test was used to assess significance; ns is not significant.
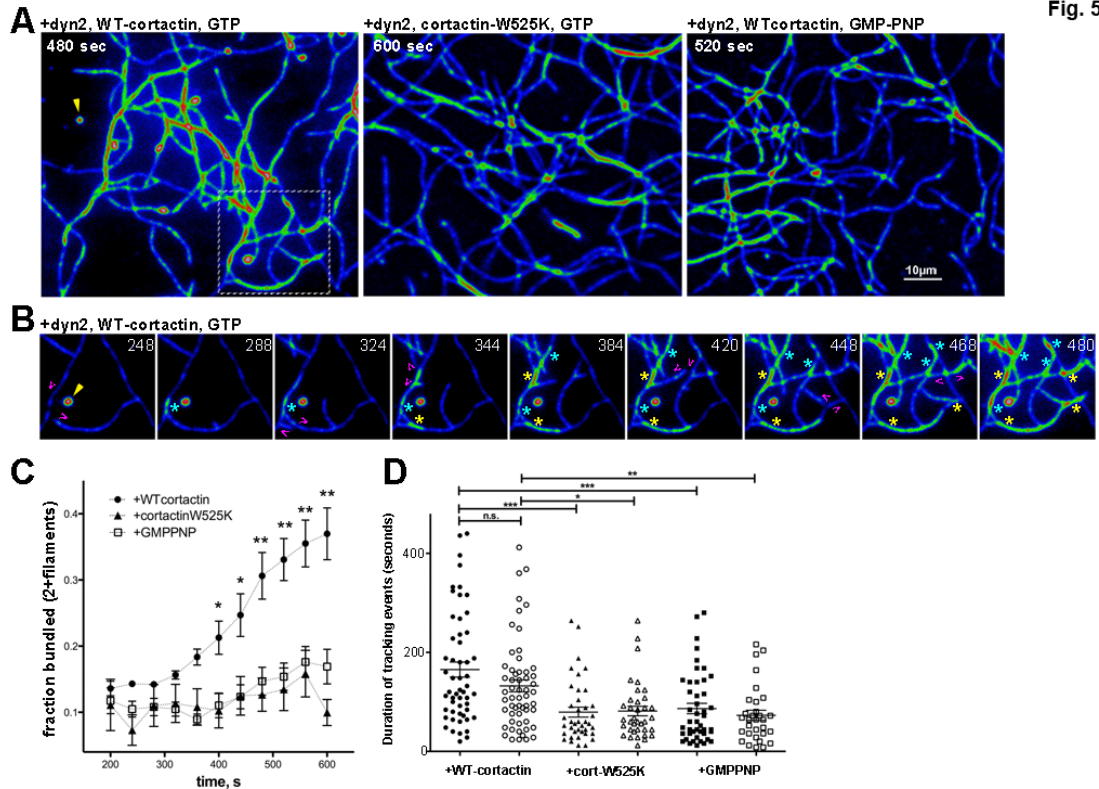
Fig. 5

Figure 5. Dyn2 and cortactin crosslink actin filaments in parallel and mixed-polarity bundles.

Panel A. TIRF micrographs of actin filaments and bundles formed after 8-10 min in reactions containing 2 µM actin (30% Alexa-488-actin), 50 nM Arp2/3 complex, 2 nM GST-VCA, 400 nM dyn2, with 400 nM cortactin or cortactin-W525K and either 1.5 mM GTP or GMPPNP, as indicated. Images are pseudocolored to indicate single actin filaments (blue), 2-filament bundles (green) and bundles containing 3 or more filaments (red). Yellow arrowhead marks an actin-containing punctum typically observed in reactions containing dyn2 and cortactin. The boxed region is shown as timelapse images in Panel **B.** Data are representative of three independent reactions containing dyn2, cortactin and GTP; one reaction was performed for samples containing either cortactin-W525K or GMPPNP. The timelapse sequence for the reaction with dyn2, cortactin and GTP is shown in **Video5a**.

Panel B. Timelapse images of boxed region of Panel A from a reaction containing dyn2, cortactin and GTP. Magenta V-shaped structures indicate actin filament barbed ends just prior to collision and elongation and tracking as a bundled segment; asterisks indicate bundles in which filaments are aligned in parallel (cyan) or anti-parallel (yellow) orientations. Yellow arrowhead marks an actin-containing punctum as described above.

Panel C. Plotted is the fraction of bundled F-actin structures (mean±SEM) with 2-or more- filaments over time. Data were obtained from three regions of interest in timelapse movies of reactions shown in **A.** Data were analyzed using one-way ANOVA with Tukey's comparison of pairwise samples. *p<0.05, **p<0.01, specified for data in which

significant differences were indicated between samples containing dyn2, cortactin and GTP and those with either cort-W525K or GMPPNP.

Panel D. Plotted is the duration in seconds of filament tracking events. Solid symbols denote parallel tracking events and open symbols denote anti-parallel tracking events for reactions shown in Panel **A**. Error bars represent the mean±SEM for 124 (dyn2+GTP), 82 (dyn2+cort-W525K) or 76 (dyn2+GMPPNP) tracking events. Data were analyzed using a two-tailed Student's *t*-test. *p<0.01, **p<0.001, ***p<0.0001, n.s., not significant
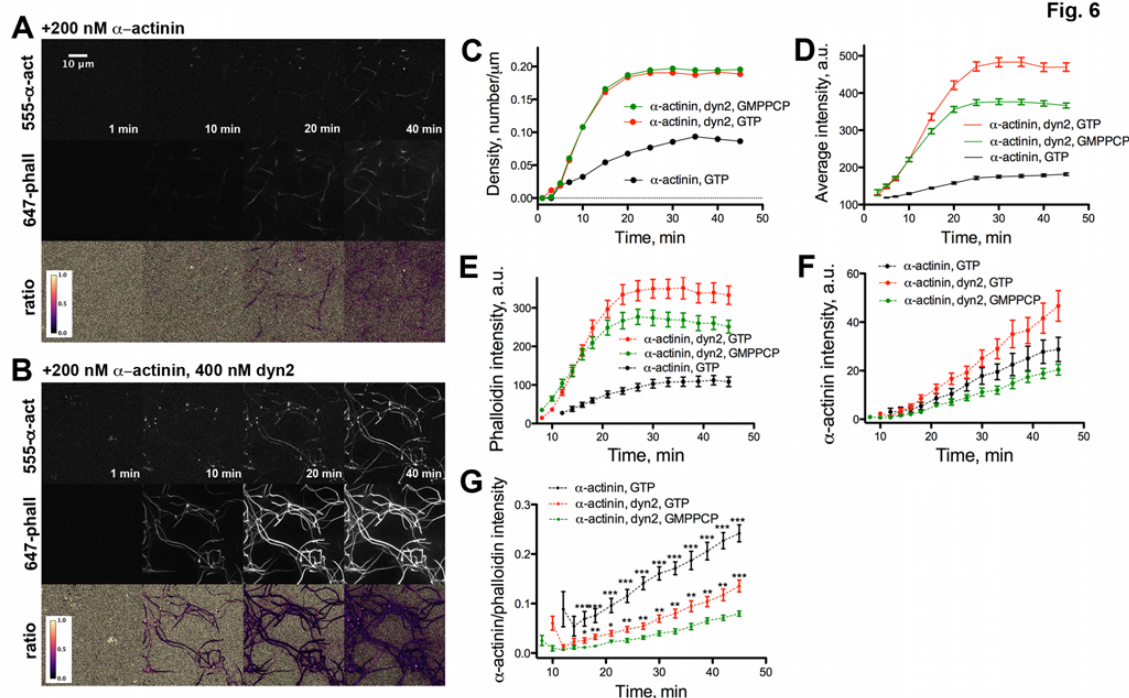
Figure 6. Dyn2-dependent bundles are restricted in binding α-actinin.

Panel A. Confocal micrographs of actin networks formed over time in a reaction containing 2.5 μM actin, 50 nM Arp2/3, 400 nM cortactin, 200 nM Alexa-555-α-actinin, 250 nM Alexa 647-phalloidin and 1.5 μM GTP. Upper and middle rows show fluorescence of Alexa-555-α-actinin and Alexa-647-phalloidin, as indicated. Lower row shows the ratio of the intensities of Alexa-555-α-actinin and Alexa-647-phalloidin. Ratios are displayed in pseudo-color according to the bar (inset). Timelapse sequences for these data are shown in **Video6a**; timelapse of ratios are shown in **Video6b**.

Panel B. Confocal micrographs of actin networks formed over time in a reaction similar to that described for Panel **A** and also containing 400 nM dyn2. Upper and middle rows show fluorescence of Alexa-555-α-actinin and Alexa-647-phalloidin, as indicated. Lower row shows the ratio of the intensities of Alexa-555-α-actinin and Alexa-647-phalloidin. Ratios are displayed in pseudo-color according to the bar (inset).

Panel C. Plotted is bundle density over time for data from timelapse movies of reactions shown in Panels **A** and **B**. Confocal micrographs of timelapse images for a reaction containing dyn2, α-actinin and GMPPCP are in **Fig. S6**.

Panel D. Plotted is the intensity of Alexa-647-phalloidin fluorescence bundles over time for data from timelapse movies of reactions shown in Panels **A** and **B** and **Fig. S6.**

Panels E-F. Plotted are the intensities of Alexa-647-phalloidin fluorescence (**E**) and Alexa-555- α-actinin fluorescence (**F**) measured along individual segments of bundles over time. Data are presented as mean±SEM for 10 bundles in each condition.

Panel G. Plotted is the ratio of the intensities of Alexa-555-α-actinin and Alexa-647-phalloidin in bundles analyzed in panels **E** and **F**. One-way ANOVA was used to assess significant differences among the three samples; ***$p<0.001$. To assess statistical significance for reactions containing dyn2 with GTP or GMPPCP, a two-tailed Student's

t-test was used; *p<0.05, **p<0.01. Data are representative of results from three independent experiments; 10 bundles were measured for each condition.

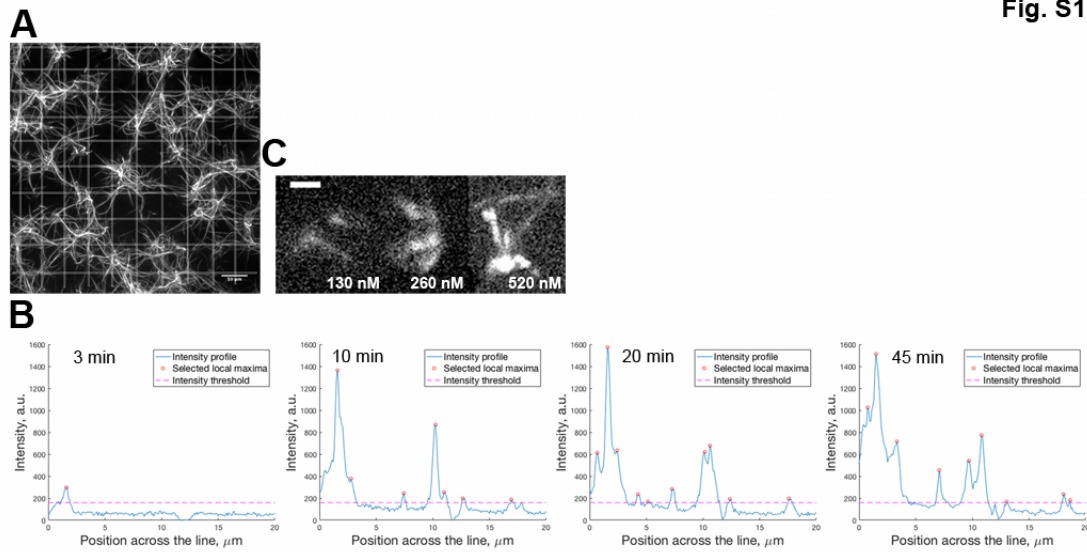**Figure S1. Analysis of F-actin bundling in reconstituted networks.**

Panel A. Micrograph a reconstituted actin network formed in the presence of 520 nM dyn2. The grid pattern indicates the set of lines used to obtain intensity profiles of Alexa647-phalloidin fluorescence for analysis of bundle density over time and the intensity of Alexa647-phalloidin fluorescence in bundled structures over time.

Panel B. A Matlab routine identified bundled structures in each line scan based on prominence of local fluorescence intensity maxima of Alexa647-phalloidin above a threshold intensity (dotted line). The local maximal intensities along each line are defined as bundles (marked by circles).

Panel C. Images of some of the earliest F-actin structures detected by 2 min in reactions containing 130 nM, 260 nM, or 520 nM dyn2, as indicated. Scale bar, 2 μm.
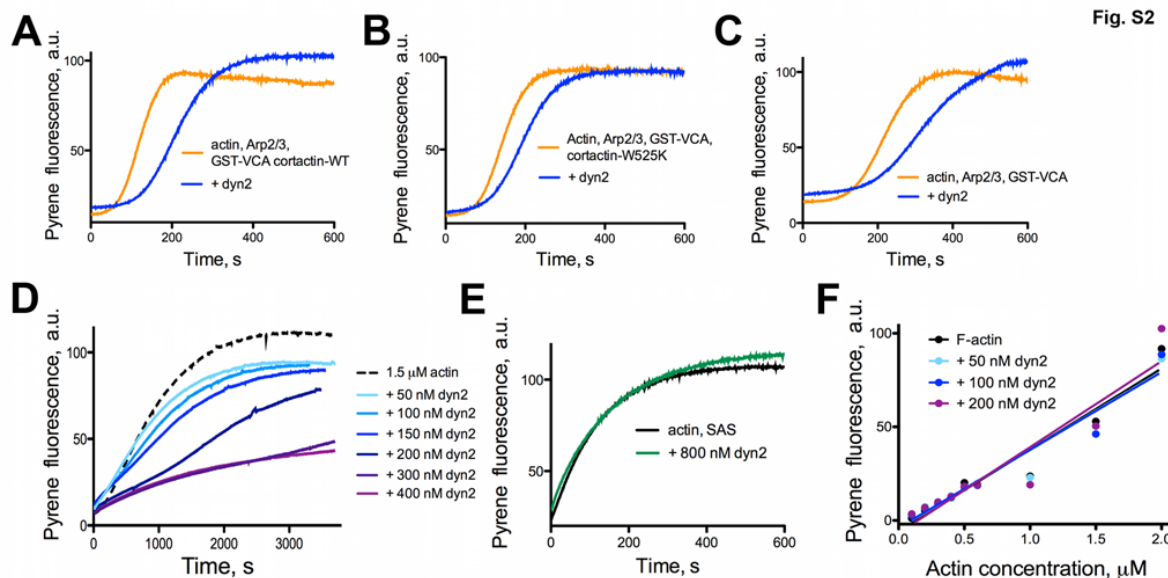
Figure S2. Dyn2 inhibits actin nucleation by Arp2/3 complex and spontaneous actin assembly.

Panels A-C. Dyn2 inhibits actin nucleation by Arp2/3 complex via a mechanism that is independent of its interaction with cortactin. Plotted is the fluorescence of pyrenyl-actin over time in reactions containing 1.5 μM actin (10% pyrene-labeled), 20 nM Arp2/3, 5 nM GST-VCA, with or without 400 nM dyn2, as indicated, and in the presence of 400 nM WT cortactin (**A**), cortactin-W525K (**B**) or in the absence of cortactin (**C**). Data are representative of results of two independent experiments.

Panel D. Dyn2 inhibits spontaneous actin assembly in a dose-dependent manner. Plotted is fluorescence of pyrenyl-actin over time in reactions containing 1.5 μM actin (10% pyrene-labeled) and varying concentrations of dyn2, as indicated.

Panel E. Dyn2 does not inhibit elongation of filaments nucleated by spectrin-F-actin seeds. Plotted is fluorescence of pyrenyl-actin over time in reactions containing 2 μM actin (10% pyrene labeled), 0.2 nM spectrin F-actin seeds (SAS) with and without 800 nM dyn2, as indicated.

Panel F. Dyn2 does not alter the critical concentration for actin assembly. Plotted is the steady-state fluorescence of pyrenyl-actin with increasing concentrations of actin (10% pyrene-labeled) in the presence varying concentrations of dyn2, as indicated. Data are representative of results of two independent experiments.
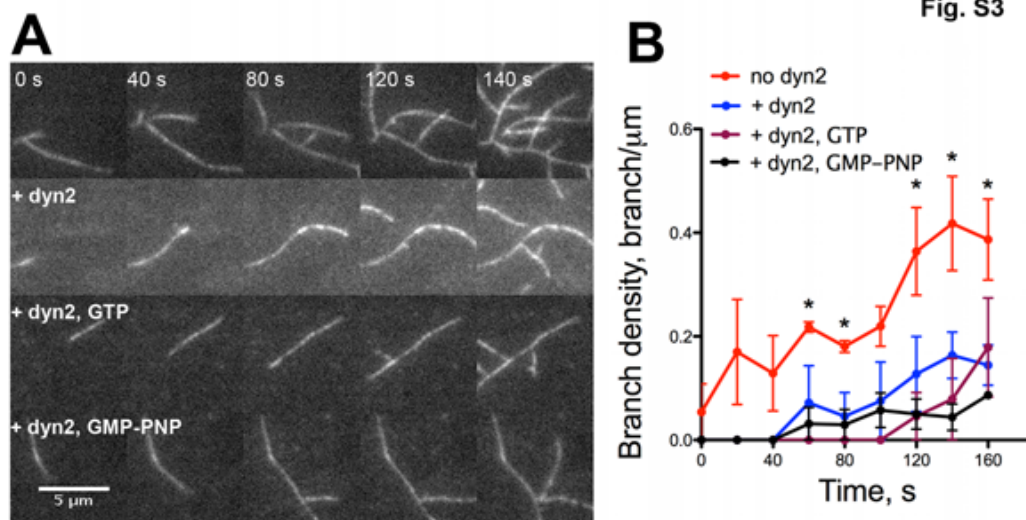
Figure S3. Inhibition of branched actin nucleation by dyn2 is independent of cortactin.

Panel A. Images from timelapse movies of actin filaments formed in reactions containing 1.5 µM actin (30% Alexa 488-labeled), 20 nM Arp2/3, 3 nM GST-VCA, with and without 200 nM dyn2, and with 1 mM of GTP, GMPPNP or no guanine nucleotide, as indicated. Data were collected using TIRM microscopy.

Panel B. Plotted is branch density over time for data collected from timelapse movies shown in Panel **A.** Bars indicate mean±SEM for at least three regions of interest from each acquisition period. Data are representative of three independent experiments. One-way ANOVA was used to determine statistically significant differences among all samples. *$p < 0.05$
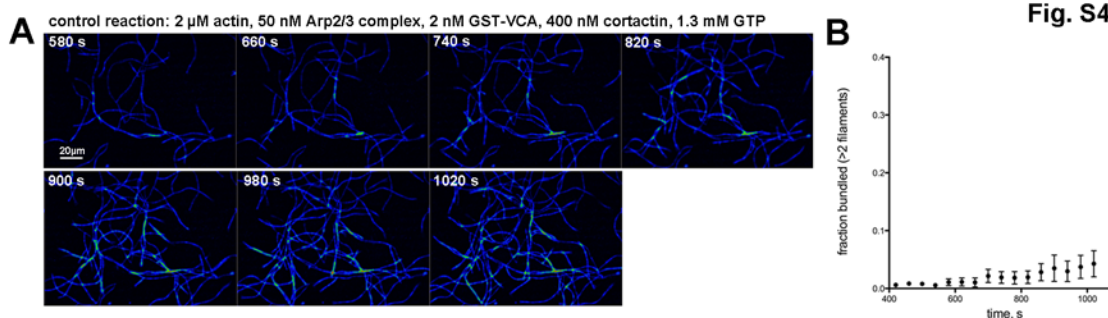
Fig. S4

Figure S4. Filament interactions in reactions containing Arp2/3 complex, GST-VCA and cortactin, but lacking dyn2 are rare and transient.

Panel A. Images from a timelapse movie collected using TIRF microscopy of a reaction containing 2 µM actin (30% Alexa-488-actin), 50 nM Arp2/3 complex, 400 nM cortactin and 1.5 mM GTP. Images are pseudo-colored to indicate single actin filaments (blue), 2-filament bundles (green) and bundles containing 3 or more filaments (red). Few filament interactions occurred prior to 9 min, thus this sequence begins 580 s after mixing. **Video5b** shows the entire timelapse sequence.

Panel B. Plotted is the fraction of bundled structures (mean±SEM) containing at least 2 filaments formed over time. Data were obtained from three regions of interest in timelapse movies of the reaction shown in **A.**
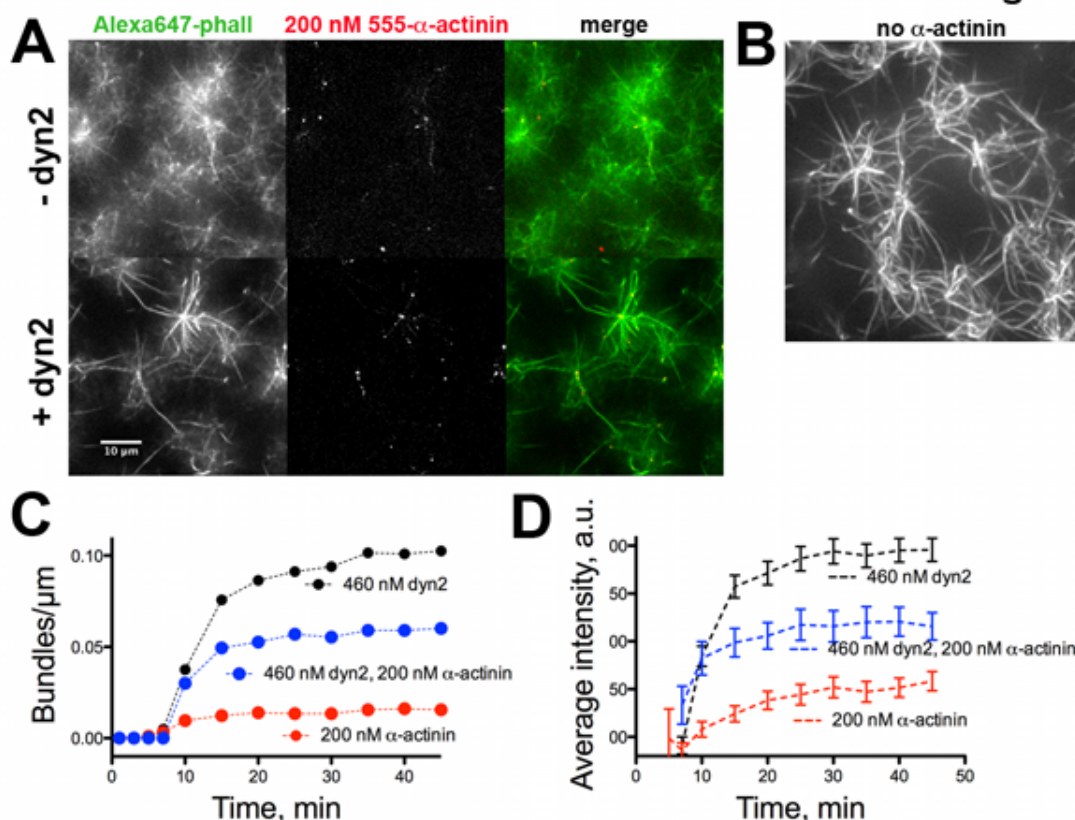
Figure S5. Branched nucleation activity interferes with bundling by α-actinin.
Panel A. Confocal micrographs of reconstituted F-actin networks formed after 20 min in reactions containing 2.5 μM actin, 50 nM Arp2/3, 2 nM GST-VCA, 400 nM cortactin, 1.5 mM GTP, 250 nM Alexa647-phalloidin, with or without 400 nM dyn2, as indicated, and 200 nM Alexa555-α-actinin. The merged pseudo-color images show Alexa555-α-actinin (red) and Alexa 647-phalloidin (green).
Panel B. Confocal micrograph of the reconstituted actin network formed after 20 min in a control reaction containing 460 nM dyn2 and lacking α-actinin. The reaction contained 2.5 μM actin, 50 nM Arp2/3, 2 nM GST-VCA, 400 nM cortactin, 1.5 mM GTP, 250 nM Alexa647-phalloidin, and 460 nM dyn2.
Panel C. Plotted is bundle density over time for data from timelapse movies shown in Panels **A and B**. Dyn2 was used at 460 nM and Alexa555-α-actinin was used at 200 nM, as indicated.
Panel D. Plotted is intensity of Alexa647-phalloidin fluorescence (mean±SEM) of bundles over time for data from timelapse movies shown in Panels **A and B**. Dyn2 was used at 460 nM and Alexa555-α-actinin was used at 200 nM.
Data are representative of results of two independent experiments. The total number of bundles (at 20 min) was 26 in reaction containing only 200 nM Alexa555-α-actinin, 75 in reaction containing 200 nM Alexa555-α-actinin and 460 nM dyn2 and 161 in reaction containing only 460 nM dyn2.
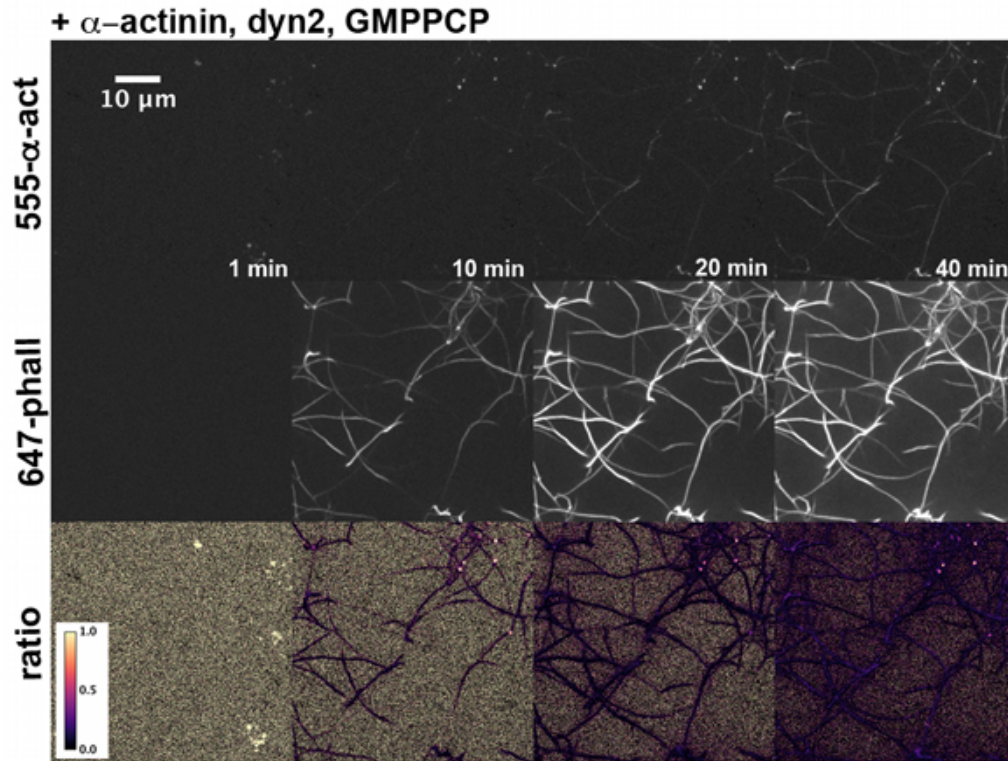
Figure S6. Dyn2 GTPase activity modulates the binding of α-actinin to dyn2-dependent bundles.

Confocal micrographs of actin network formed over time in a reaction containing 2.5 μM actin, 50 nM Arp2/3, 400 nM cortactin, 200 nM Alexa555-α-actinin, 400 nM dyn2, 250 nM Alexa647-phalloidin and 1.5 mM GMPPCP. Upper and middle rows show fluorescence of Alexa555-α-actinin and Alexa647-phalloidin, as indicated. Lower row shows the ratio of the intensities of Alexa555-α-actinin and Alexa647-phalloidin. Ratios are displayed in pseudo-color according to the bar (inset). Data shown are representative of three independent experiments.

Supplementary movie legends

Video1. Dyn2 bundles filaments in reconstituted Arp2/3 complex-dependent actin networks. Timelapse images displayed as projected z-stacks of actin networks formed in reactions containing 2.5 µM actin, 50 nM Arp2/3, 2 nM GST-VCA, 400 nM cortactin, 1.5 mM GTP and 250 nM Alexa647-phalloidin, with increasing concentrations of dyn2, as indicated, were acquired every minute by confocal microscopy. Gain setting for the movie with no dyn2 is enhanced to highlight network features; all other panels are displayed using identical settings. The rate of playback is 8 frames per second (fps); the timestamp references the start of imaging.

Video2. Interactions of the cortactin SH3 domain and the dyn2 proline-rich domain (PRD) are required for filament bundling in reconstituted branched actin networks. Timelapse images displayed as projected z-stacks of actin networks formed in reactions containing 2.5 µM actin, 50 nM Arp2/3, 2 nM GST-VCA, 1.5 mM GTP, 250 nM Alexa647-phalloidin, 400 nM dyn2, and with 400 nM of either WT cortactin or mutant cortactin-W525K, as indicated, were acquired every minute by confocal microscopy. The rate of playback is 8 fps; the timestamp references the start of imaging.

Video3. Dyn2 and cortactin bundle spontaneously assembled actin networks. Timelapse images displayed as projected z-stacks of actin networks formed in reactions containing 2.5 µM actin, 1.5 mM GTP, 250 nM Alexa647-phalloidin, 400 nM dyn2, and with 400 nM of either WT cortactin or mutant cortactin-W525K, as indicated, or lacking cortaction. Images were acquired every minute by confocal microscopy. The rate of playback is 8 frames per second (fps); the timestamp references the start of imaging.

Video4. GTPase activity by dyn2 regulates bundled network morphology. Timelapse images of actin networks formed in reactions containing 2.5 µM actin, 50 nM Arp2/3, 2 nM GST-VCA, 400 nM cortactin, 400 nM dyn2 and 250 nM Alexa647-phalloidin, with 1.5 mM GTP, GMPPCP or without nucleotide, as indicated, were acquired every minute by confocal microscopy. The rate of playback is 8 frames per second (fps); the timestamp references the start of imaging.

Video5a. Dyn2 and cortactin bundle actin filaments in parallel and mixed-polarity bundles. Timelapse images of actin filaments formed in a reaction containing 2 µM actin (30% Alexa-488-actin), 50 nM Arp2/3 complex, 400 nM dyn2, 400 nM cortactin 1.3 mM GTP were acquired every 4 s by TIRF microscopy. Images are pseudo-colored to indicate single actin filaments (blue), 2-filament bundles (green) and bundles containing 3 or more filaments (red). The movie is played at a rate of 12 fps; the timestamp references the start of the reaction.

Video5b. Actin filaments interact transiently in reactions lacking dyn2. Timelapse images of actin filaments formed in a reaction containing 2 µM actin (30% Alexa-488-

actin), 50 nM Arp2/3 complex, 400 nM cortactin 1.3 mM GTP, were acquired every 4 s by TIRF microscopy. Images are pseudo-colored to indicate single actin filaments (blue), 2-filament bundles (green) and bundles containing 3 or more filaments (red). Rate of playback is 12 fps; the timestamp references the start of the reaction.

Video6a. Dyn2-dependent bundles are restricted in binding α-actinin.
Timelapse images displayed as projected z-stacks of actin networks formed in reactions containing 2.5 μM actin, 50 nM Arp2/3, 400 nM cortactin, 200 nM Alexa-555-α-actinin, 250 nM Alexa 647-phalloidin and 1.5 μM GTP, with and without 400 nM dyn2, as indicated. The fluorescence of Alexa-555-α-actinin (red) and Alexa-647-phalloidin (green) are merged; images were acquired every 1 min. The rate of playback is 8 fps; the timestamp references the start of imaging.

Video6b. Ratio image sfor timelapse sequences of bundled networks formed in reactions containing either only α-actinin or dyn2+ α-actinin. This sequence shows the ratio of the intensities of Alexa555-α-actinin and Alexa647-phalloidin over time for timelapse images shown in **Video6a**. Movie playback is 8 fps; the timestamp references the start of imaging.

Chapter 3. Discussion and future directions

Summary

How actin filament networks change their organization to support cellular processes and structures is not completely understood. For example, some studies suggest that branched F-actin networks in lamellipodia reorganize to assemble lamellar actomyosin structures (Burnette et al., 2011; Hotulainen and Lappalainen, 2006); however, we still do not understand how branched filaments assemble into bundled structures. Using biochemical and microscopic assays *in vitro*, I showed that (1) by decreasing the extent of branching in Arp2/3 complex-dependent networks, dyn2 potentiates filament bundling. (2) Dyn2, in complex with cortactin, promotes formation of F-actin bundles that selectively bind α-actinin. (3) Dyn2 GTPase activity changes structural properties of filament bundles. These findings support the idea that dyn2 and cortactin specify the architecture of branched F-actin networks in lamellipodia to promote assembly of actomyosin at the lamella. In the following sections, I propose a mechanism by which dyn2 and cortactin organize lamellipodial networks to promote actomyosin assembly and describe the weaknesses of the model and the future directions of this research.

A model for dyn2-dependent mechanism of actomyosin assembly at the lamella from branched networks in lamellipodia

As nascent actomyosin forms at the edge of the migrating cell, bundled actin filaments are thought to co-assemble with myosin II to form transverse arcs near the lamellipodia-lamella interface (Beach et al., 2017; Burnette et al., 2011; Fenix et al., 2016; Hotulainen and Lappalainen, 2006). However, because lamellipodial networks exist as branched, crosslinked arrays of actin filaments, they either need to be remodeled

into bundled structures (for example, by severing or de-branching) or unbranched filaments should be generated *de novo* to form F-actin bundles in lamellipodia. In my experiments, dyn2 inhibited branched nucleation by Arp2/3 complex to promote formation of unbranched filaments, and a dyn2-cortactin complex formed filament bundles that selectively bind α-actinin within reconstituted branched networks. These findings are consistent with the idea that dyn2 and cortactin arrange *de novo* generated filaments as bundles that assemble contractile transverse arcs at the lamella **(Fig. 1)**.

In U2-OS cells, dyn2 localizes to the edge of advancing lamellipodial protrusions (Menon et al., 2014). Because ring-like dyn2 oligomers directly bind F-actin *in vitro* (Gu et al., 2010), I propose that assembled dyn2 rings bind a subset of filaments within protruding lamellipodia and locally inhibit branched nucleation by Arp2/3 complex to create unbranched actin filaments **(Fig 1a)**. As previously observed, dyn2 and cortactin bundle actin filaments *in vivo* and *in vitro* (Mooren et al., 2009; Yamada et al., 2016). Therefore, I propose that dyn2 interacts with cortactin to create a collection of short bundled filaments (a "bundle template") in lamellipodia **(Fig 1b)**. Cortactin crosslinks branched actin filaments *in vitro* (Helgeson et al., 2014). Additionally, my experiments showed that dyn2/cortactin bundles expand by elongating and accumulating F-actin along the bundles. Therefore, a bundle template may expand by adding actin filaments crosslinked by cortactin and by adding new dyn2-cortactin complexes **(Fig. 1c)**. Because dyn2 is only enriched at the edge of advancing lamellipodial protrusions (Menon et al., 2014), I propose that dyn2 is released from the bundles as they flow toward the lamellipodia-lamella interface, whereas cortactin continues to crosslink bundled structures **(Fig 1d)**. As bundled structures flow toward the lamella, they begin to co-

assemble with myosin II filaments, but are not crosslinked by α-actinin because dyn2/cortactin bundles delay crosslinking by α-actinin **(Fig. 1e).** As cortactin is released at the lamellipodia-lamella interface, myosin bundles begin to accumulate α-actinin to assemble transverse arcs at the lamella **(Fig. 1f)**.

This model is supported by data from dyn2-depleted U2-OS cells (Menon et al., 2014). When dyn2 is depleted, transverse arcs assemble at the lamella, but they do not efficiently engage with focal adhesions, which results in an increased rate of myosin II retrograde flow. This phenotype may result from the fact that, without dyn2, actin filaments of nascent transverse arcs may be crosslinked by α-actinin as subsets of isotropic meshwork, rather than continuous bundles, which prevents efficient coupling with focal adhesions due to their inability to exert tension on focal adhesions.
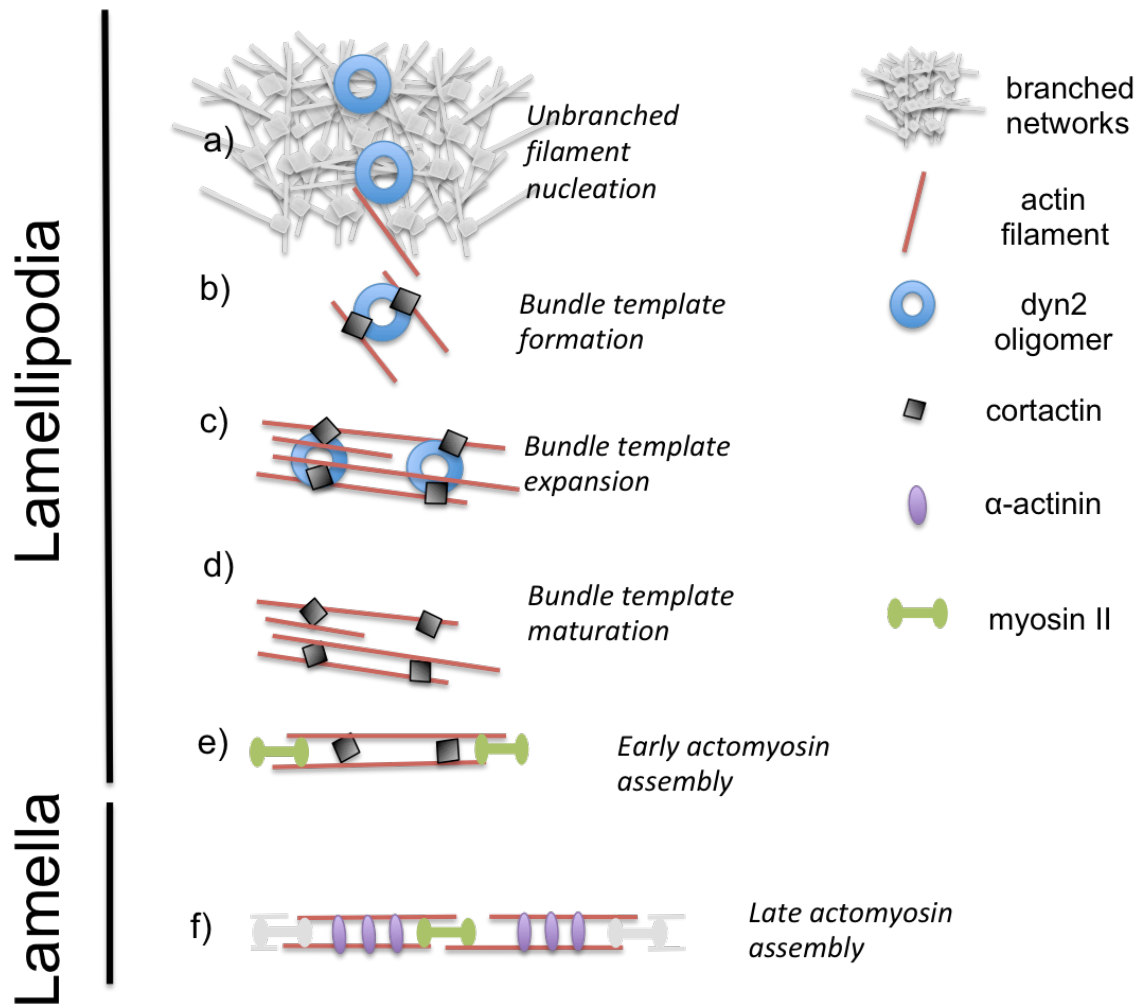
Figure 1. Proposed mechanism for lamellar actomyosin assembly from lamellipodial networks potentiated by dyn2.

a) *Unbranched filament nucleation*. Dyn2 oligomers assemble at the edge of advancing lamellipodia; they locally decrease branched nucleation to create unbranched filaments.

b) *Bundle template formation*. Dyn2 interacts with cortactin to assemble a collection of short crosslinked filaments (a "bundle template").

c) *Bundle template expansion*. Bundle templates expand by nucleating filaments along the bundles and by elongating and crosslinking filaments within bundles by additional dyn2-cortactin complexes.

d) *Bundle template maturation*. As bundle templates flow toward the lamella, dyn2 is released; cortactin still crosslinks the bundles.

e) *Early actomyosin assembly*. As bundles move closer to the lamellipodia-lamella interface, myosin filaments begin co-assembling with the bundle templates.

f) *Late actomyosin assembly*. At the lamellipodia-lamella interface, cortactin is released from the bundles and is replaced by α-actinin. As a result, contractile actomyosin bundles (transverse arcs) emerge at lamella.

Proposed role for the GTP cycle in dyn2-dependent effects on lamellipodial F-actin networks

The mechanism dynamin's GTPase cycle is derived primarily from biochemical assays with unassembled dynamin molecules, experiments with dynamin oligomers assembled on lipid templates, and from data on the crystal structure of dynamin in the presence of various nucleotides (Antonny et al., 2016). Dynamin assembles into a helical structure surrounding a lipid tubule (Sweitzer and Hinshaw, 1998). Interaction between two G domains in adjacent rungs of the dynamin helix creates a trans-dimer. GTP binding results in constriction of the lipid tubules (Zhang and Hinshaw, 2001). Upon GTP hydrolysis, dynamin oligomer undergoes a conformational change within the bundle signaling element through a change in relative positions of trans-G domains. GDP and inorganic phosphate are released upon GTP hydrolysis at an unknown rate (Antonny et al., 2016).

In solution, dynamin oligomers disassemble upon GTP hydrolysis (Warnock et al., 1996). GTPase activity by dynamin is stimulated by phospohoinositides and the SH_3 domain-containing proteins, such as cortactin and grb2 through interaction with dynamin's PH domain and PRD, respectively (Barylko et al., 1998; Mooren et al., 2009). Interestingly, the most potent effector of dynamin's GTPase activity is its own self-assembly, which stimulates GTPase activity as much as 10-fold (Warnock et al., 1996).

Based on these data and my experiments that show that addition of GTP regulates F-actin bundle formation by dyn2, I propose that dyn2's GTPase activity first changes the conformation of a dyn2 oligomer to stabilize cortactin's ability to crosslink actin filaments. This is followed by a release of dyn2 from the bundle by disassembling the

oligomer. In this way, dyn2 is recycled once the bundle template is formed. Once dyn2 is released from the bundle, it quickly undergoes another round of assembly and can be reused as an F-actin crosslinker.

Challenges to the proposed model

While my model of actomyosin assembly from branched lamellipodial networks is supported by experimental data, there are several weaknesses of the model that have not been addressed.

First, although dynamin oligomers were previously visualized on F-actin bundles (Gu et al., 2010; Yamada et al., 2013), my experiments have not studied whether dyn2 is localized on bundles, whether it functions as an oligomer, and whether dyn2 and cortactin form a complex that bundles actin filaments. Further, I showed that dyn2 GTPase activity influences bundle network morphology and crosslinking by α-actinin; however, the exact function of GTP hydrolysis in modulating the dyn2 function is not clear. Experiments aimed to address these issues are presented as future directions.

Second, based on the *in vivo* data that dyn2 depletion affects actomyosin assembly in U2-OS cells (Menon et al., 2014), my model assumes that dyn2 and cortactin potentiate formation of bundle templates to assemble transverse arcs at the lamella. However, my experiments did not address the role of dyn2 in actomyosin assembly. Experiments that will study how dyn2 affects actomyosin assembly are proposed as future directions of this research.

Additionally, while my research shows that the interaction between dyn2 and cortactin is required for bundle formation, Gu et al. (2010) show that dynamin1 can

directly bundle F-actin *in vitro*. Future experiments are needed to explain this discrepancy.

Finally, I propose a mechanism by which dyn2 can tune the architecture of branched F-actin networks to potentiate the formation of bundled structures. This mechanism can be relevant for different actin structures across the cell; however, my experiments were performed with reconstituted proteins *in vitro*. Therefore, future experiments are warranted to test and refine my model in dyn2-dependent actin structures and processes across the cell.

Future directions

Future experiments presented here will test different aspects and predictions of my model and assess its physiological relevance.

To determine where dyn2 and cortactin are situated on F-actin bundles within the network of bundled filaments and assess the dynamics of their binding to F-actin, one could fluorescently label these proteins and visualize their interactions with actin filaments using TIRF microscopy. Both dyn2 and cortactin bind actin filaments (Gu et al., 2010; Helgeson and Nolen, 2013). Therefore, I expect the complex of these proteins to bind unbundled actin filaments, and one could analyze their dynamics as they assemble filament bundles. It is important to test whether the dyn2-cortactin complex is targeted preferentially to branch points or along filament sides. My model predicts that, while cortactin alone preferentially binds branched filaments at their branch points (Helgeson and Nolen, 2013), the complex of dyn2 and cortactin should have higher affinity for unbranched filaments. To address this point, one could measure the "on" and "off" rate

and the lifetime of each protein and the dyn2-cortactin complex on branched and unbranched filaments.

To study the role of GTP hydrolysis in bundling actin filaments by dyn2 and cortactin, one could compare kinetics of dyn2-cortactin binding in the presence of different guanine nucleotides. In my experiments, addition of a non-hydrolyzable GTP analog (GMPPCP) caused networks of bundled filaments to appear less interconnected and have shorter bundles, suggesting that GTP hydrolysis releases dyn2 from the bundle and recycles it. Therefore, I expect dyn2 and/or cortactin to stay longer on bundles (or have a decreased "off" rate) when GMPPCP is used compared to GTP.

Finally, some studies suggest that dynamin can directly bind F-actin and bundle it (Gu et al., 2010). Although my experiments indicate that cortactin is necessary for bundling F-actin, dyn2 directly inhibited actin nucleation. Therefore, it is necessary to determine if dyn2 directly binds actin filaments and bundles by observing interactions of labeled dyn2 with actin filaments using TIRF microscopy.

My research proposed a new function for dyn2 and cortactin in specifying assembly of bundled actin filaments that restrict crosslinking by α-actinin. I propose that bundle templates assembled by dyn2 and cortactin may co-assemble with myosin II filaments in lamellipodia to promote actomyosin formation within the lamella; however, I did not perform experiments that address interactions of myosin II with dyn2-dependent bundled networks. Therefore, the next step should be to reconstitute actomyosin networks that include fluorescently labeled myosin II with or without dyn2. These experiments will answer the question: Does dyn2/cortactin-dependent bundles promote formation of actomyosin structures? If my hypothesis is correct, I expect to observe increased myosin

II associated with bundled filaments in the presence of dyn2 and cortactin compared to the condition without dyn2 or cortactin.

To observe actomyosin assembly in dyn2/cortactin-dependent bundled networks, one could use a micropattern system used to study actin regulation *in vitro* (Reymann et al., 2010). In this system, branched actin is nucleated on a glass surface in shapes (for example, rods) specified by printed NPF patterns. The rate of actomyosin contractility can be assessed by comparing the extent of deformation of actomyosin structures assembled on the patterns (Reymann et al., 2012). It would be interesting to determine if contractile activity differs in networks assembled with and without dyn2. Based on my hypothesis that dyn2/cortactin bundles promote actomyosin assembly, I expect that addition of dyn2 will increase the rate of network deformation.

It is important to use cellular systems to confirm results obtained *in vitro*. To test a role of dyn2 and cortactin in actomyosin assembly *in vivo*, I propose using live cell imaging to visualize actomyosin assembly in live U2-OS cells. Studying actin dynamics in live cells is challenging due to a high density of actin filaments in lamellipodia, but super-resolution microscopy techniques can overcome this issue by increasing the spatial resolution. One such approach, structured illumination microscopy (SIM), was used to observe the dynamics of myosin II assembly in live U2-OS cells (Fenix et al., 2016). This technique visualizes (with ~110 nm resolution) individual assemblies of myosin II filaments. I propose using U2-OS cells depleted or not of dyn2 to observe actomyosin assembly using SIM. Based on my model, I expect to detect "abnormal" actomyosin assembly (decreased kinetics of assembly of myosin II minifilaments, decreased association of myosin with actin filaments, or disorganized actin filaments) when dyn2 is

depleted. To address the role of dyn2 and cortactin in actomyosin assembly, one needs to identify a specific region of the dyn2 PRD that binds cortactin and generate a mutant to rescue dyn2 knockdown in U2-OS cells. Because my experiments show that the interaction of dyn2 and cortactin is necessary for filament bundling, I expect this mutant to perturb actomyosin assembly at the lamella.

It is often challenging to separate dyn2 endocytic function from its effects on F-actin. However, a growing body of evidence suggests that the role of dyn2 in endocytosis stems, at least partially, from its effects on actin cytoskeleton. Future studies are needed to determine a general mechanism by which dyn2 regulates F-actin in endocytosis. In yeast, a dynamin homolog, Vps1, bundles actin filaments to promote vesicle scission (Palmer et al., 2015). Of note, yeast does not express a cortactin homolog, and Vps1 bundles actin filaments through a direct interaction with actin or through other actin-binding proteins, such as Abp1 (Goode et al., 2001). These data indicate that F-actin bundling is important for scission during endocytosis. My *in vitro* experiments suggest that dyn2 and cortactin form bundle templates capable of organizing F-actin bundling. I speculate that elongation of filaments within bundle templates formed at the neck of clathrin-coated pits applies pushing forces at the membrane to promote vesicle scission **(Fig. 2)**; however information to identify how actin filaments associate with dyn2 must be obtained to propose a more comprehensive mechanism. To test my hypothesis, one could visualize bundle templates *in vivo*, which can be done by super-resolution microscopy or electron microscopy in U2-OS cells undergoing endocytosis. Cells should be depleted of dyn2 and rescued with wild type dyn2, dyn2-K5E5 (an actin-binding mutant), or dyn2 mutant that does not bind cortactin. I expect to detect actin bundles at

the neck of the clathrin-coated pit in cells carrying the wild type dyn2, but not the
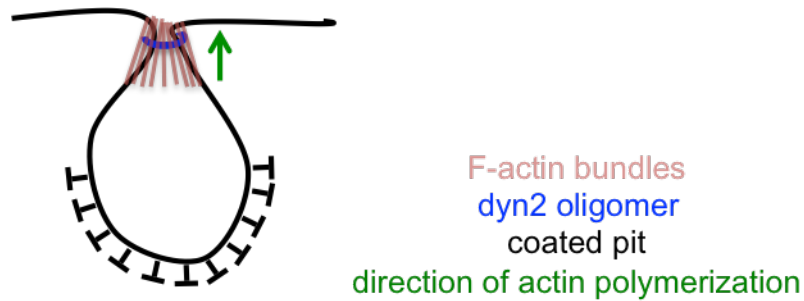
cortactin and/or actin-binding mutant.

F-actin bundles
dyn2 oligomer
coated pit
direction of actin polymerization

Figure 2. Schematic representation of proposed actin regulation by dyn2 during endocytosis in yeast. Dynamin oligomer (blue) is assembled around the clathrin-coated pit (black) as a ring or a spiral. Actin-binding regions in the stalk domain interact with actin and create a bundle template that elongates toward the plasma membrane and applies pushing forces that promote vesicle fission from the membrane.

Beyond endocytosis, dyn2 is enriched in other actin structures that depend on Arp2/3 complex. Interestingly, some of these structures are organized into bundles, despite their dependence on the Arp2/3 complex activity, such as filopodia, actin comets, podosomes/invadopodia, and protrusions formed during myoblast fusion (Destaing et al., 2013; Orth et al., 2002; Shin et al., 2014; Yamada et al., 2013). Although an interaction of dyn2 with cortactin has only been shown in filopodia, cortactin and dyn2 regulate assembly of actin comets and podosomes and both are enriched at the sites of cell-cell fusion (Orth et al., 2002; Oser et al., 2009; Takito et al., 2012). Therefore, it is possible that dyn2 and cortactin regulate the transition of branched F-actin networks into bundles within different F-actin structures in the cell. Super-resolution and electron microscopy techniques that visualize actin bundles within these structures combined with dyn2 and cortactin depletion and mutants that disrupt dyn2-actin and dyn2-cortactin binding will be useful in addressing the role of dyn2 and cortactin in these processes.

Concluding remarks

My research established that dyn2 interferes with branch nucleation by Arp2/3 complex to promote the assembly of bundled filaments. Bundled filaments bind α-actinin in a GTPase-dependent manner. Based on my data, I propose a mechanism for assembly of F-actin bundles by dyn2 and cortactin in the context of branched Arp2/3 complex-dependent networks that can be important for several F-actin-dependent processes and structures in the cell. It is necessary to refine the model and test its predictions *in vitro*

and *in vivo* in order to dissect the mechanism by which dyn2 remodels actin filament

networks in different parts of the cell.

References

Beach, J.R., Bruun, K.S., Shao, L., Li, D., Swider, Z., Remmert, K., Zhang, Y., Conti, M.A., Adelstein, R.S., Rusan, N.M., et al. (2017). Actin dynamics and competition for myosin monomer govern the sequential amplification of myosin filaments. Nat. Cell Biol. *19*, 85–93.

Barylko B., Binns D., Lin K.M., Atkinson M.A., Jameson D.M., Yin H.L., Albanesi J.P. (1998) Synergistic activation of dynamin GTPase by Grb2 and phosphoinositides. J Biol Chem. *273*, 3791-3797.

Burnette, D.T., Manley, S., Sengupta, P., Sougrat, R., Davidson, M.W., Kachar, B., and Lippincott-Schwartz, J. (2011). A role for actin arcs in the leading-edge advance of migrating cells. Nat. Cell Biol. *13*, 371–381.

Destaing, O., Ferguson, S.M., Grichine, A., Oddou, C., De Camilli, P., Albiges-Rizo, C., and Baron, R. (2013). Essential Function of Dynamin in the Invasive Properties and Actin Architecture of v-Src Induced Podosomes/Invadosomes. PLoS One *8*, e77956.

Fenix, A.M., Taneja, N., Buttler, C.A., Lewis, J., Van Engelenburg, S.B., Ohi, R., Burnette, D.T., and Engelenburg, S.B. Van (2016). Expansion and concatenation of non-muscle myosin IIA filaments drive cellular contractile system formation during interphase and mitosis. Mol. Biol. Cell *27*, 1–29.

Gu, C., Yaddanapudi, S., Weins, A., Osborn, T., Reiser, J., Pollak, M., Hartwig, J., and Sever, S. (2010). Direct dynamin-actin interactions regulate the actin cytoskeleton. EMBO J. *29*, 3593–3606.

Helgeson, L. A., and Nolen, B.J. (2013). Mechanism of synergistic activation of Arp2/3 complex by cortactin and N-WASP. eLife *2*, e00884.

Helgeson, L.A., Prendergast, J.G., Wagner, A.R., Rodnick-smith, M., and Nolen, B.J. (2014). Interactions with Actin Monomers , Actin Filaments , and Arp2 / 3 Complex Define the Roles of WASP Family Proteins and Cortactin in Coordinately Regulating Branched Actin. J. Biol. Chem. *289*, 28856-28869

Hotulainen, P., and Lappalainen, P. (2006). Stress fibers are generated by two distinct actin assembly mechanisms in motile cells. J. Cell Biol. *173*, 383–394.

Menon, M., Askinazi, O.L., and Schafer, D.A. (2014). Dynamin2 organizes lamellipodial actin networks to orchestrate lamellar actomyosin. PLoS One *9*, e94330.

Mooren, O.L., Kotova, T.I., Moore, A.J., and Schafer, D.A. (2009). Dynamin2 GTPase and cortactin remodel actin filaments. J. Biol. Chem. *284*, 23995–24005.

Orth, J.D., Krueger, E.W., Cao, H., and McNiven, M. A. (2002). The large GTPase dynamin regulates actin comet formation and movement in living cells. Proc. Natl. Acad. Sci. *99*, 167–172.

Oser, M., Yamaguchi, H., Mader, C.C., Bravo-Cordero, J.J., Arias, M., Chen, X., DesMarais, V., Van Rheenen, J., Koleske, A.J., and Condeelis, J. (2009). Cortactin regulates cofilin and N-WASp activities to control the stages of invadopodium assembly and maturation. J. Cell Biol. *186*, 571–587.

Palmer, S.E., Smaczynska-de Rooij, I.I., Marklew, C.J., Allwood, E.G., Mishra, R., Johnson, S., Goldberg, M.W., and Ayscough, K.R. (2015). A Dynamin-Actin Interaction Is Required for Vesicle Scission during Endocytosis in Yeast. Curr. Biol. *25*, 868–878.

Reymann, A.-C., Martiel, J.-L., Cambier, T., Blanchoin, L., Boujemaa-Paterski, R., and Théry, M. (2010). Nucleation geometry governs ordered actin networks structures. Nat. Mater. *9*, 827–832.

Reymann, A.-C., Boujemaa-Paterski, R., Martiel, J.-L., Guérin, C., Cao, W., Chin, H.F., De La Cruz, E.M., Théry, M., and Blanchoin, L. (2012). Actin network architecture can determine myosin motor activity. Science *336*, 1310–1314.

Shin, N.-Y., Choi, H., Neff, L., Wu, Y., Saito, H., Ferguson, S.M., De Camilli, P., and Baron, R. (2014). Dynamin and endocytosis are required for the fusion of osteoclasts and myoblasts. J. Cell Biol. *207*, 73–89.

Sweitzer S.M., Hinshaw J.E. (1998) Dynamin undergoes a GTP-dependent conformational change causing vesiculation. Cell. *93*, 1021-1029.

Takito, J., Nakamura, M., Yoda, M., Tohmonda, T., Uchikawa, S., Horiuchi, K., Toyama, Y., and Chiba, K. (2012). The transient appearance of zipper-like actin superstructures during the fusion of osteoclasts. J. Cell Sci. *125*, 662–672.

Warnock D.E., Hinshaw J.E., Schmid S.L. (1996) Dynamin self-assembly stimulates its GTPase activity. J Biol Chem. *271*, 22310-22314.

Yamada, H., Abe, T., Satoh, A., Okazaki, N., Tago, S., Kobayashi, K., Yoshida, Y., Oda, Y., Watanabe, M., Tomizawa, K., et al. (2013). Stabilization of Actin Bundles by a Dynamin 1/Cortactin Ring Complex Is Necessary for Growth Cone Filopodia. J. Neurosci. *33*, 4514–4526.

Yamada, H., Takeda, T., Michiue, H., Abe, T., and Takei, K. (2016). Actin bundling by dynamin 2 and cortactin is implicated in cell migration by stabilizing filopodia in human non-small cell lung carcinoma cells. Int. J. Oncol. *49*, 877–886.

Zhang P., Hinshaw J.E. (2001) Three-dimensional reconstruction of dynamin in the

constricted state. Nat Cell Biol. *3*, 922-926.